TRACKING ERROR ANALYSIS FOR SATELLITE SURVEILLANCE SYSTEMS

Chester J. Kurys, et al

Massachusetts Institute of Technology

Prepared for:

Electronic Systems Division
Advanced Research Projects Agency

29 April 1974

UNCLASSIFIED

Security Classification

AD-779 918

DOCUMENT CONTROL DATA - R&D

(Security classification of title, body of abstract and indexing annotation must be entered when the overall report is classified)

1. ORIGINATING ACTIVITY *(Corporate author)* Lincoln Laboratory, M.I.T.	2a. REPORT SECURITY CLASSIFICATION Unclassified 2b. GROUP

3. REPORT TITLE

Tracking Error Analysis for Satellite Surveillance Systems

4. DESCRIPTIVE NOTES *(Type of report and inclusive dates)*

Technical Note

5. AUTHOR(S) *(Last name, first name, initial)*

Kurys, Chester J. and Steinway, William J.

6. REPORT DATE	7a. TOTAL NO. OF PAGES	7b. NO. OF REFS
29 April 1974	94	2

8a. CONTRACT OR GRANT NO. F19628-73-C 0002 b. PROJECT NO. ARPA Order 600 c. d.	9a. ORIGINATOR'S REPORT NUMBER(S) Technical Note 1974-28 9b. OTHER REPORT NO(S) *(Any other numbers that may be assigned this report)* ESD-TR-74-168

10. AVAILABILITY/LIMITATION NOTICES

Approved for public release; distribution unlimited.

11. SUPPLEMENTARY NOTES	12. SPONSORING MILITARY ACTIVITY
None	Advanced Research Projects Agency, Department of Defense

13. ABSTRACT

The problem of determining preliminary orbit parameters of a previously unobserved satellite using several types of postulated space surveillance systems has been investigated.

The space surveillance systems used in this analysis are ground-based optics (single-and dual-telescope systems), two ground-based radar systems each with a different capability, and a satellite-borne tracking sensor. The Non-Real-Time Precision Orbit Determination (NRTPOD) Program was used as the analysis tool. The study is restricted to satellites whose perigee altitude is above 7500 km. An analysis of a typical Molniya orbit is included as a special case.

The capabilities of each sensor system are studied for specific orbits.

14. KEY WORDS

tracking error analysis | satellite surveillance systems | sensor systems

I

UNCLASSIFIED

Security Classification

MASSACHUSETTS INSTITUTE OF TECHNOLOGY
LINCOLN LABORATORY

TRACKING ERROR ANALYSIS FOR SATELLITE SURVEILLANCE SYSTEMS

C. J. KURYS
Group 31

W. J. STEINWAY
KREMS

TECHNICAL NOTE 1974-28

29 APRIL 1974

LEXINGTON MASSACHUSETTS

The work reported in this document was performed at Lincoln Laboratory, a center for research operated by Massachusetts Institute of Technology. This work was sponsored by the Advanced Research Projects Agency of the Department of Defense under Air Force Contract F19628-73-C-0002 (ARPA Order 600).

ABSTRACT

The problem of determining preliminary orbit parameters of a previously unobserved satellite using several types of postulated space surveillance systems has been investigated.

The space surveillance systems used in this analysis are ground-based optics (single-and dual-telescope systems), two ground-based radar systems each with a different capability, and a satellite-borne tracking sensor. The Non-Real-Time Precision Orbit Determination (NRTPOD) Program was used as the analysis tool. The study is restricted to satellites whose perigee altitude is above 7500 km. An analysis of a typical Molniya orbit is included as a special case.

The capabilities of each sensor system are studied for specific orbits.

Accepted for the Air Force
Eugene C. Raabe, Lt. Col., USAF
Chief, ESD Lincoln Laboratory Project Office

TABLE OF CONTENTS

I. INTRODUCTION

General purpose space surveillance systems are designed to detect and track all satellites which come into the field of view. Such systems do not depend on any acquisition aids and hence can also detect and track non-radiating payloads and space debris. In this memo the capability of several types of satellite surveillance systems to generate track data and extrapolate that data forward in time is investigated. For each system several track data rate algorithms are used to generate a sufficient amount of data to achieve useful extrapolation results. The criterion for evaluation and comparison of tracking capabilities is the positional accuracy of the satellite obtained when the track data are extrapolated forward in time.

The first consideration is the nature of short-term (fraction of an orbit period) extrapolation errors as a function of the length of the initial observation interval. For short observation intervals the errors grow rapidly during extrapolation and the target must be tracked again so that a refined orbit fit can be made. The second consideration is with long-term extrapolation errors, that is over one or more orbit periods. The long-term extrapolation results are parameterized as a function of total observation time, number of observations and measurement accuracies.

To aid in the analysis of the capability of each system, use is made of the general purpose computer program NRTPOD. The NRTPOD program has the ability to perform trajectory and orbit estimation, make position and velocity predictions for a satellite, and estimate the uncertainty in position and velocity resulting from the sensor measurement errors. It can accept real data or generate fictitious observation data, assigning measurement errors to each observation point. A trajectory or orbit is fitted to the data using a least-squares algorithm. A covariance matrix of the uncertainty in the predictions is also generated. The trajectory (orbit) and covariance matrix are then propagated forward in time to determine the position and velocity of the satellite and the associated uncertainty in those elements at various times after the observations. This analysis assumes that convergence to a minimum weighted r.m.s. residual trajectory has been accomplished.

The program has been used as a standard analytical tool for trajectory analysis at Lincoln Laboratory. It includes a sophisticated collection of

mathematical, statistical and operational techniques to produce results of high precision. In practice, simpler algorithms and colored noise measurements may produce less desirable results.

Summary

Three sensor categories are considered: ground-based optics, ground-based radar and a satellite-borne angle-only sensor. These systems were chosen for analysis on the basis of current interest and feasibility requirements. The next section describes the systems and their measurement capability.

The study concerns itself with satellites whose perigee altitude is above 7500 km. Section III gives some statistical data about targets in this altitude region. These data are used as a basis for choosing the satellite orbits for which the error analyses are conducted. The categories of orbits are: 1, 2, and 3 times synchronous-altitude circular, and near-synchronous eccentric. Not all systems were analyzed for all orbits.

Section IV, V and VI contain the descriptions of the track data rate algorithms used and the details of the error analyses for the three systems. Separate specific conclusions are given at the end of each section In terms of general conclusions, several things can be said:

1. Each sensor system is capable of developing a good ephemeris. By good is meant that the prediction accuracy is good enough to recognize the satellite on the next occasion that it becomes visible to the sensor under consideration.
2. The time to develop the ephemeris varies depending on the satellite orbit, but in all cases the observation time required is less than the available viewing window.
3. It is concluded that, judging only on the basis of this error analysis, there is no strong preference among the systems described.

II. SENSOR SYSTEMS

Three sensor categories are considered in this study. They are ground-based optics, ground-based radar and a satellite-borne angle-only sensor. The ground-based optical systems are (1) a single-telescope sensor and (2) a dual-telescope sensor consisting of two similar telescopes on a 100-km baseline. Two ground-based radar systems were considered. The first, RADAR 1, has a capability of detecting and tracking satellites up to synchronous altitudes. The second, RADAR 2, has a capability of detecting and tracking satellites between synchronous and three-times synchronous altitudes. The satellite-borne angle-only sensor is placed in a geostationary orbit with a capability of detecting and tracking satellites at ranges up to 120,000 km.

A. Ground-Based Optics

For the purposes of this memo, it is assumed that the optical systems discussed have the capability to observe satellites regardless of range considerations. Questions of satellite visibility (because of reflective properties) or optical sensitivities are not at issue in this text. The observations result in a measurement of satellite position with a specified accuracy in both right ascension and declination. The overall field of view of an optical search system is assumed to be many orders of magnitude larger than the resolution capability. The measurement accuracy is independent of sensitivity for the optical systems considered.

The first optical system is a single telescope with an accuracy of 0.001° in both angle measurements. The second system consists of two similar telescopes located 100 km apart. In this dual system both telescopes make measurements at the same time, and one data point in this system consists of two sets of two angle measurements with an accuracy of 0.001°. The dual-telescope system enables information about the range of the satellite to be available from one data point.

B. Ground-Based Radar

Two radar systems were designed to perform the search and track functions on long-range satellites. The basic parameters of RADAR 1 which

has a capability of detecting and tracking satellites at ranges up to synchronous altitude are listed in Table II-1.

TABLE II-1
RADAR 1 PARAMETERS

Beamwidth	1^{o}
Dwell Time	1.25 sec/beam pos.
Sensitivity	10 dB/dwell time @ 1 x sync altitude
Field of View	El $\geqslant 45^{o}$

Two waveforms were designed for the radar with an option to incorporate coding (10 kc bandwidth) on the pulse to study the effects of increased range resolution. The first waveform consisted of a 0.2-second-long pulse at ~48% duty cycle. This waveform was used to track satellites in near-synchronous orbit. A second waveform was designed to track satellites in highly elliptical orbits with an apogee altitude near one-times synchronous altitude. This waveform consisted of a 50-millisecond pulse (10 kc bandwidth) at a 20% duty cycle. The waveforms are shown schematically in Figure II-1.

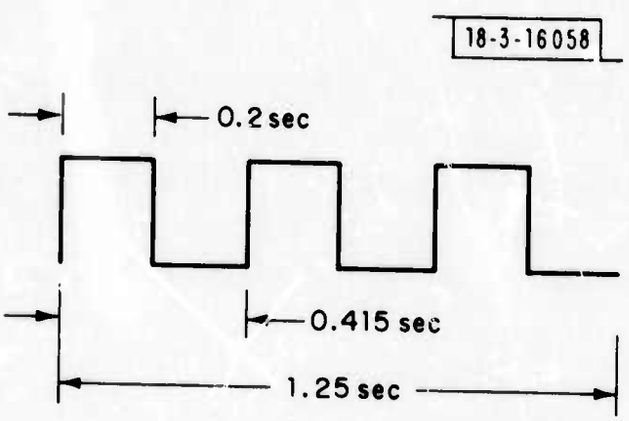

Fig. II-1a. RADAR 1 Waveform: CW Waveform

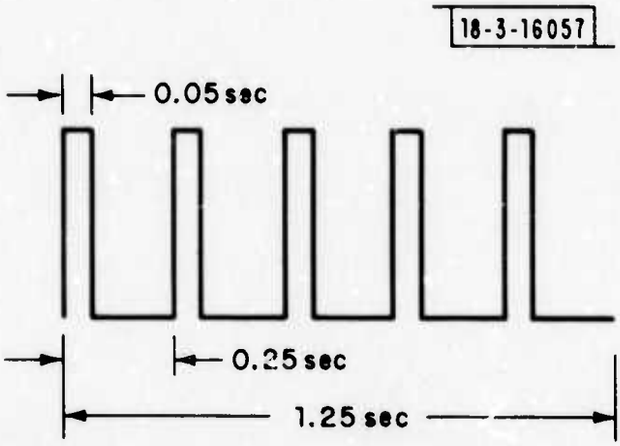

Fig. II-1b. RADAR 1 Waveform: Coded Waveform

The basic parameters of RADAR 2, which has a capability of detecting and tracking satellites at ranges up to three times synchronous altitude, are listed in Table II-2.

TABLE II-2

RADAR 2 PARAMETERS

Beamwidth	0.5°
Dwell Time	1.25 sec/beam pos.
Sensitivity	10 dB/dwell time @3 x sync altitude
Field of View	El $\geqslant$ 45°

A single waveform was designed for this radar with the option of incorporating coding (10 kc bandwidth) to study the effects of improved range resolution. This waveform consisted of a 0.25-second pulse at a 20% duty cycle. Figure II-2 shows the waveform.

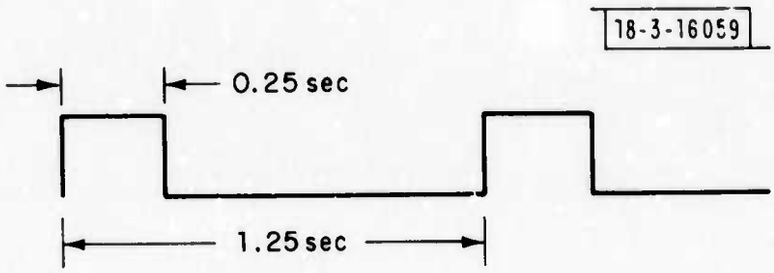

Fig. II-2. Radar 2 Waveform

These waveforms were designed to keep the peak to average power ratio low. The interpulse time is determined by the round trip time to the maximum range of interest. The first waveform has a duty cycle which may not be achieved in practice. The pulse length can be shortened with a corresponding increase in peak power. The overall results of the error analysis should not change significantly for small changes in range resolution. It is assumed that the Doppler from the returned pulse can be extracted and used as an input to the orbit determination algorithms. Furthermore, it is assumed that the three and five sub-pulses of the RADAR 1 waveforms can be coherently processed over 1 second to gain the added Doppler resolution.

C. Satellite-Borne Angle-Only Tracker

This section considers a sensor which is in a geostationary orbit defined by the following parameters.

inclination = 0

eccentricity = 0

period = period of earth's rotation

For the purposes of analysis, it is sufficient to assume that the sensor is capable of detecting and tracking a satellite at ranges up to 120, 000 km using

angle-only data and that it is not capable of measuring range or range-rate data. A cone whose half angle is 13.6°, which is equivalent to looking to within ±5° of the earth's limb, is excluded from the sensor's field of view. As a result, many low-altitude satellites are not visible to this system. The angular accuracy is 0.05° and independent of target range.

III. SATELLITE ORBITS

This study concerns itself only with satellites whose perigee altitude is above 7500 km. The data base used to determine the following statistics includes all successful launches through 1972, with perigee above 7500 km. This data base is comprised of 78 satellites whose perigee altitude is above 7500 km. Note that there are satellites whose perigee altitude is below 7500 km but apogee altitude is above 7500 km. These satellites are excluded from this analysis. It is assumed that this class of satellites does not decay very rapidly, therefore the data base is a good indication of where and how many satellites are in orbit above the perigee altitude of 7500 km. The distribution function was calculated using the following equation:

$$\text{Distribution} \equiv \frac{\text{number of satellites} \leq n\,h}{N}$$

where n = an integer

N = total number of satellite launches

h = altitude increment

The perigee and apogee distributions for satellites whose perigee altitude is above 7500 km are shown in Fig. III-1 and 2. These distributions indicate that a large number of the satellites have perigee and apogee altitudes of approximately 35,000 km; i.e., near-synchronous altitude. Figs. III-3 and 4 show the eccentricity and inclination plotted vs. orbital period. Each dot represents one satellite. If two satellites lie in very nearly identical orbits, only one dot is plotted in Figs. 3 and 4. These figures indicate that the majority of the satellites whose orbital period is approximately 86,400 seconds (1 day) have eccentricities ~ 0 and inclinations of $\sim 0°$. Another large class of satellites is seen whose perigee and apogee altitudes are approximate 120,000 km. These satellites exhibit an eccentricity of ~ 0 and inclination of $\sim 36°$. There is a small number of satellites with large eccentricities, $e > 0.7$.

The satellite orbits chosen for analysis in this study fall into the general categories cited above. They are meant to be representative of what

exists and by no means are they to be considered complete nor to represent a worst case orbit for each of the sensor systems. Table III-1 is a matrix of the satellite orbits used along with the orbital elements.

TABLE III-1

SATELLITE ORBITS

Satellite Orbit Designation	OSCULATING CLASSICAL ELEMENTS					
	a (km)	e	i (Deg)	Ω (Deg)	ω (Deg)	M (Deg)
1 x	40,000	0	0	0	0	0
2 x	80,000	0	36.0	0	0	0
3 x	120,000	0	36.0	0	0	0
1 x → 3 x	80,000	0.5	0	0	0	0
Molniya	26,554	0.72	62.9	229	318.4	72.2
SYNC	42,164.2	0	0	0	0	0

The SYNC orbit case was chosen for analysis by the angle-only tracking sensor in geostationary orbit. This target will appear at a fixed range and angle relative to the orbiting sensor. The rates (range and angle) of the target relative to the sensor are zero. Table III-2 is a matrix of the satellite orbits analyzed for each sensor.

TABLE III-2

SENSORS AND ORBITS

Sensor	Orbits					
	1 x	2 x	3 x	1 x→3 x	Molniya	SYNC
1 Telescope	X		X			
2 Telescopes	X		X			
RADAR 1	X				X	
RADAR 2			X	X		
Satellite-Borne Tracker		X	X		X	X

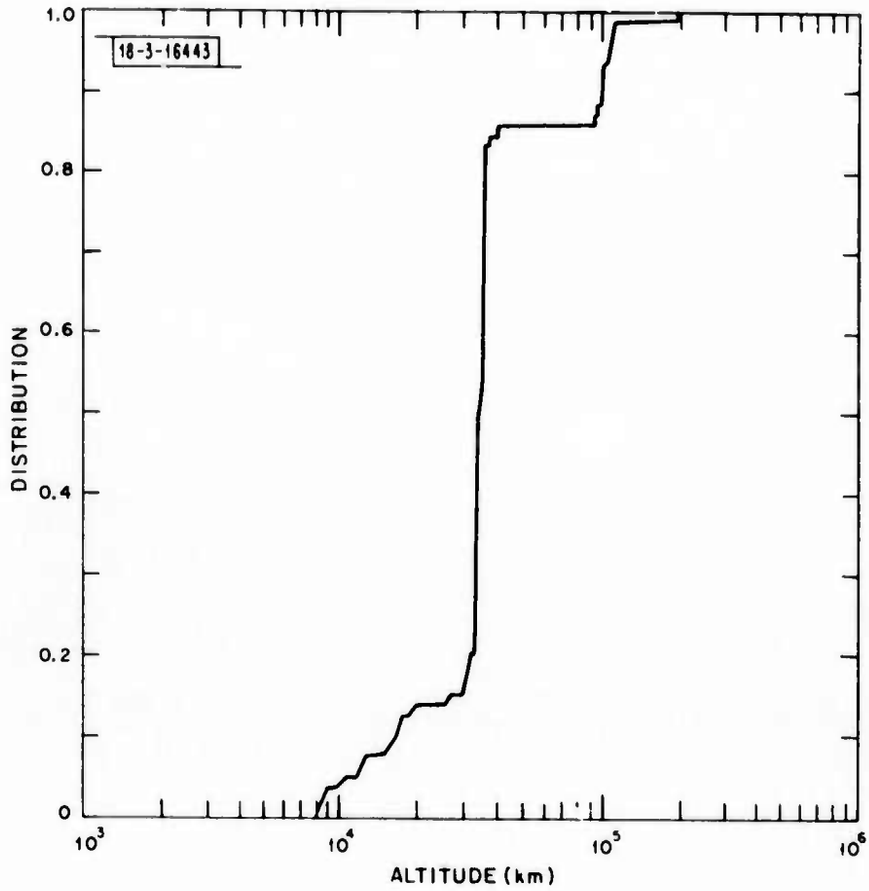

Fig. III-1. Perigee Distribution vs. Altitude (for Satellites with Perigee above 7500 km)

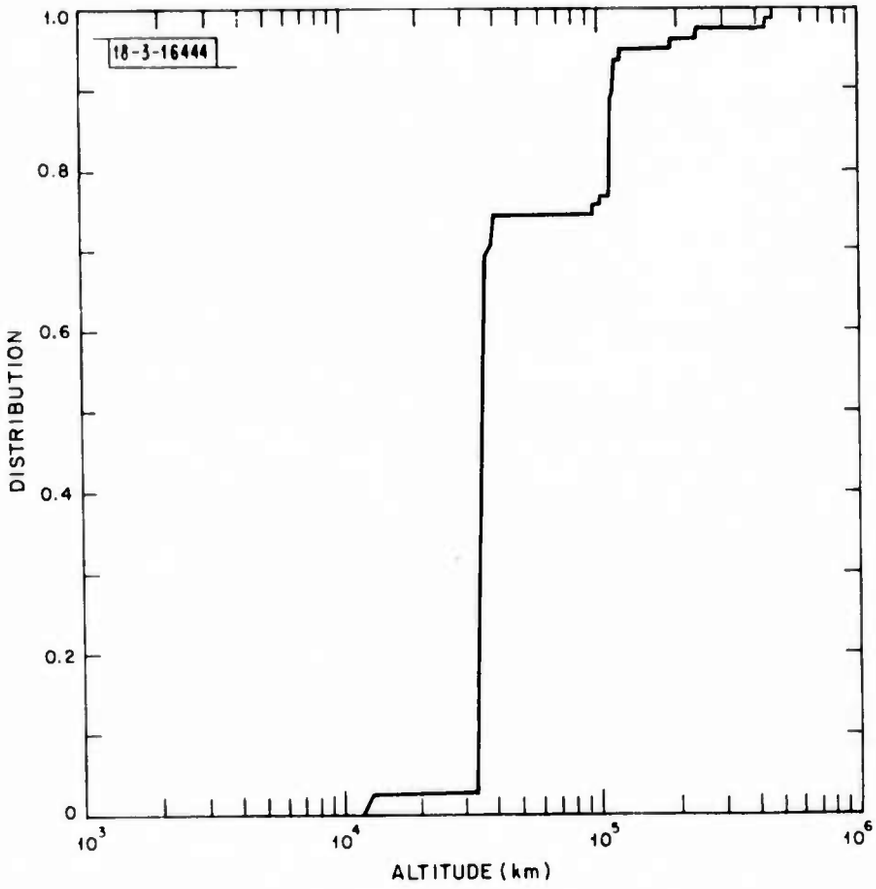

Fig. III-2. Apogee Distribution vs. Altitude (for Satellites with Perigee above 7500 km)

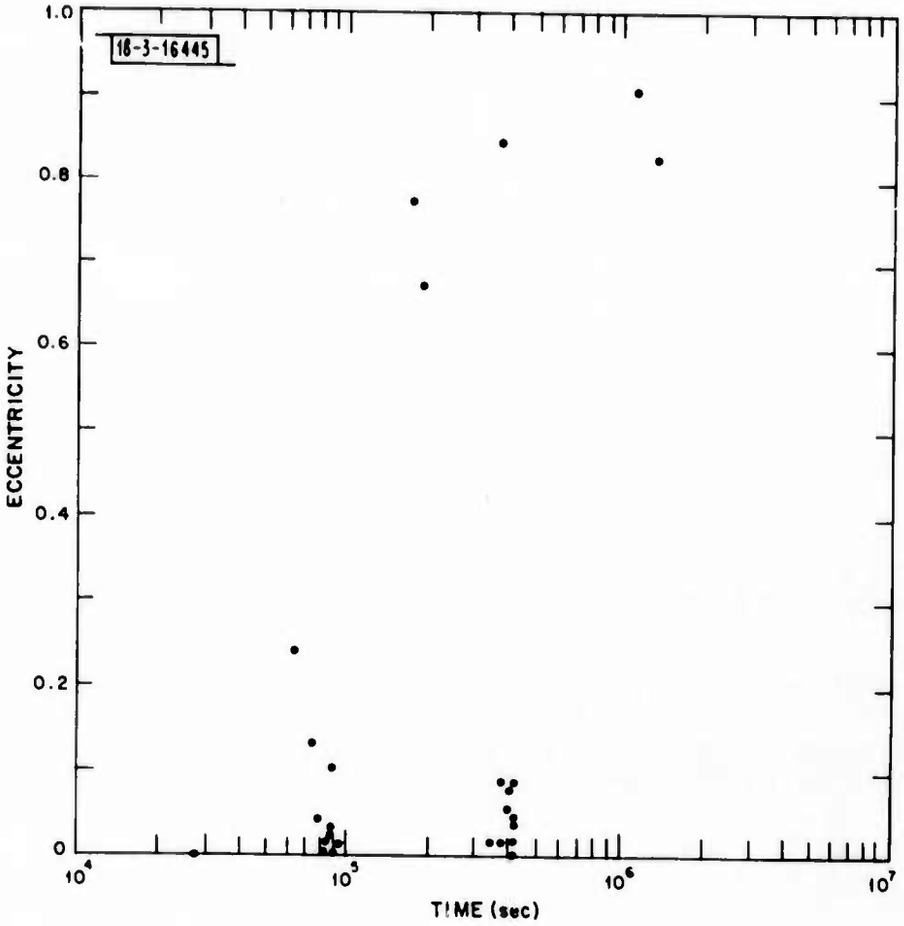

Fig. III-3. Eccentricity vs. Orbital Period (for Satellites with Perigee above 7500 km)

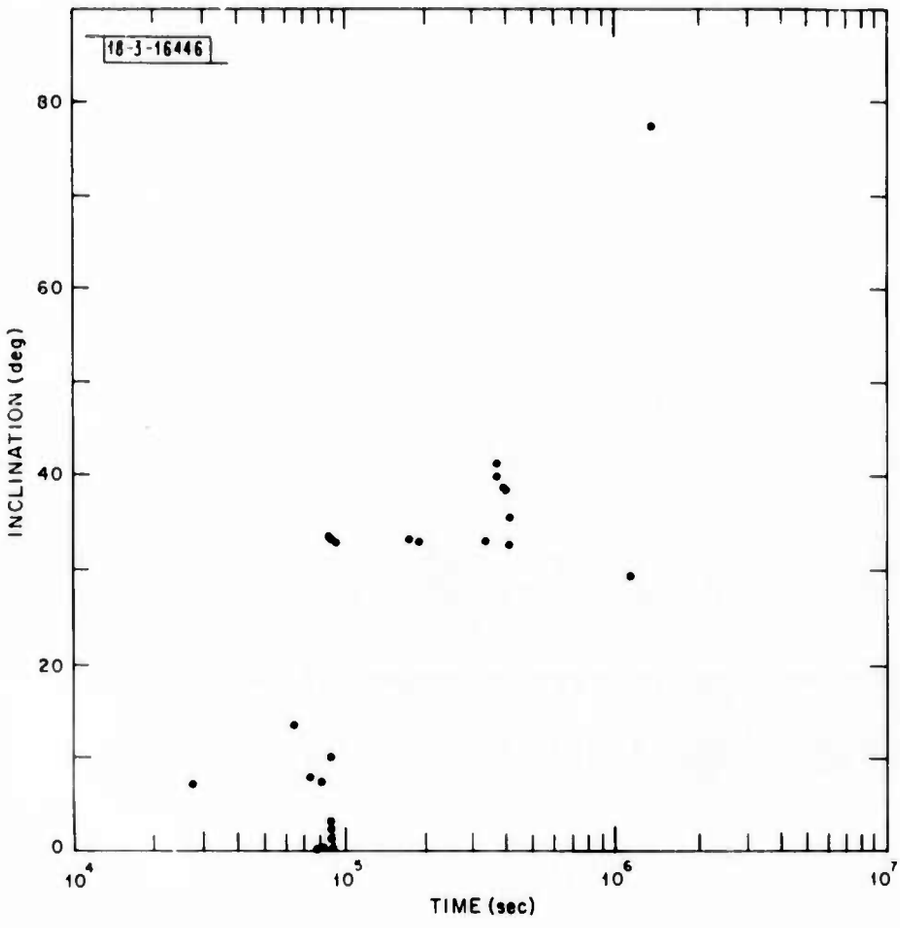

Fig. III-4. Inclination vs. Orbital Period (for Satellites with Perigee above 7500 km)

IV. GROUND-BASED-OPTICS ERROR ANALYSIS

The first concern is the nature of short-term extrapolation errors as a function of the length of the initial observation interval. Fig. IV-1 illustrates the geometry for the situation. The short-term observation interval, δt_1, simulates the first detection and subsequent tracking of a satellite to obtain the initial trajectory estimate. Using the NRTPOD simulation program, a set of observations and associated accuracies are generated. The error analysis routines then propagate the measurement uncertainties forward in time to establish an error volume along the nominal trajectory. For short observation intervals the errors grow rapidly, and the satellite must be tracked again so that a refined orbit fit can be made. The choice of time, ΔT, when the next observation interval occurs, is most affected by the sensor field of view, the length of the initial observation interval, δt, and sensor measurement uncertainties. The short-term results are presented as a function of these parameters.

The second concern is the long-term extrapolation of errors, that is over one or more orbit periods. Several short-term observation intervals may be made, and these are used to compute a refined set of orbit parameters. The results of the long-term extrapolation are parameterized as a function of the time between short-term observation intervals, ΔT, and the number of intervals, N.

The following results are first categorized by short-term and long-term extrapolation, and then by orbits, one-time-synchronous and three-times-synchronous. The comparison of the single-and double-telescope systems is made only in the short-term extrapolation cases.

A. Short-Term Observations

The first case is the one-times-synchronous-altitude orbit, circular, with a semi-major axis of 40,000 km. To provide the effects of a variation of observation time on extrapolated errors, observation intervals of 4, 8, 12, and 20 minutes were used. Using a computer simulation, several evenly spaced, individual data points (angle measurements) were taken during the observation interval. In principle, it is only necessary to take a

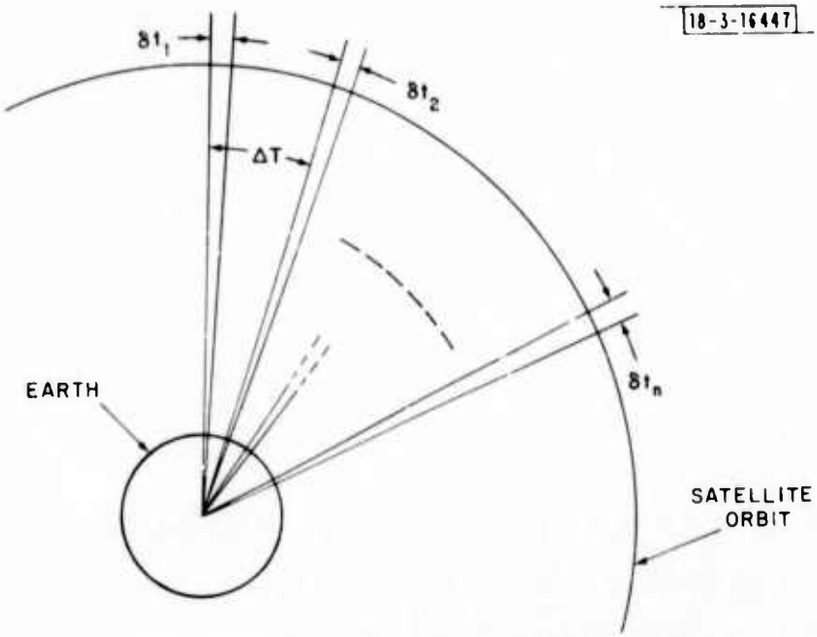

δt_i = SHORT INTERVAL OVER WHICH DATA SET IS TAKEN

n = TOTAL NUMBER OF DATA SETS

ΔT = SHORT-TERM EXTRAPOLATION

$(n-1) \times \Delta T$ = TOTAL INTERVAL OVER WHICH OBSERVATIONS ARE GATHERED

Fig. IV-1. Optical Sensor - Definitions

"minimal data set" over the observation interval, i.e., three observations of two angles each. To insure proper conditioning of parameters in the NRTPOD error propagation algorithm 9 data points were used in the simulation. The geometry of the observations has been conceptually indicated in Figure IV-1. For the 1x sync orbit (a=40,000 km, e=0, i=0°) the sensor is located at 30° N, 160° W with the satellite starting at 170° E. For the 3 x sync orbit (a = 120,000 km, e = 0, i = 36°) the sensor is located at 30° N, 230° W with the satellite starting at 30° N and 155° E. The single sensor and dual, 100-km-baseline, sensor have measurement accuracies of 0.001° in angle and the results in the following can be scaled directly as the measurement accuracy. Figures IV-2 and 3* plot the standard deviation of error in elevation and azimuth (sensor coordinates) versus extrapolation time for the single and dual sensor systems respectively.

If, for example, the sensor field of view is 1° x 1°, and the system is required to maintain a probability of > 98% of acquiring the satellite ΔT minutes in the future, then a standard deviation of angular error allowable, σ_A, is 0.2° in azimuth and elevation. Table IV-1 summarizes, and allows comparison between, the two sensor systems for σ_A = 0.2° and 1°. It is evident that in this error analysis the benefits of the dual sensor are slight for the 1 x synchronous orbit.

The second case is the three-times-synchronous altitude orbit, circular, with a semi-major axis of 120,000 km. To provide the effects of a variation of observation time on extrapolated errors, intervals of 5, 10, 20, and 60 minutes were used. Figs. IV-4 and 5 plot the results and Table IV-2 provides a summary and comparison of the two sensor systems. The benefits of the dual sensor are clearly indicated for the 3x synchronous orbit by the increased extrapolation time. The dips in azimuth prediction error occurring at 150 min. on Fig. IV-5 occur because the long slender steadily growing error ellipsiod in 3 dimensions is oriented perpendicular to the direction of increasing azimuth at that time.

---

* The time origin for the plots is the beginning of the observation interval.

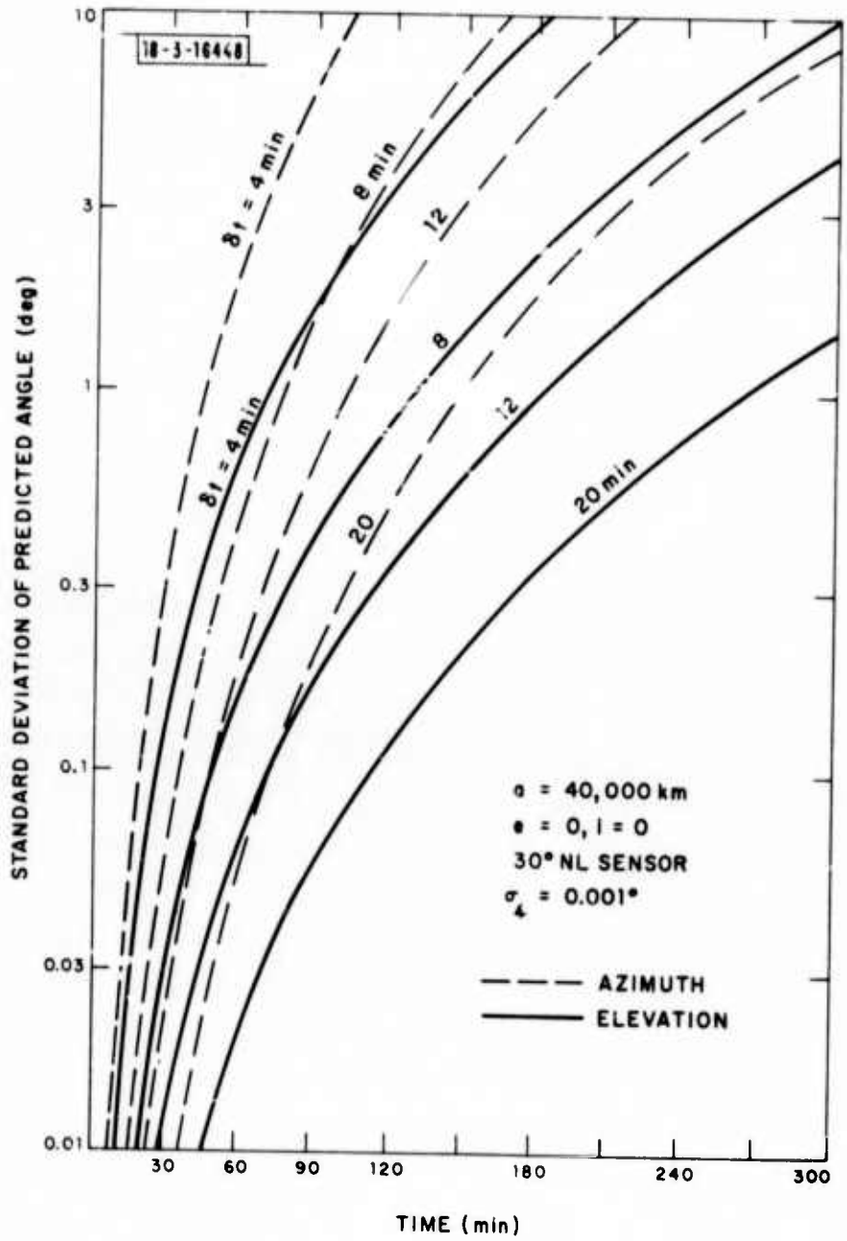

Fig. IV-2. Single Sensor, 1 x Sync., Short Extrapolation

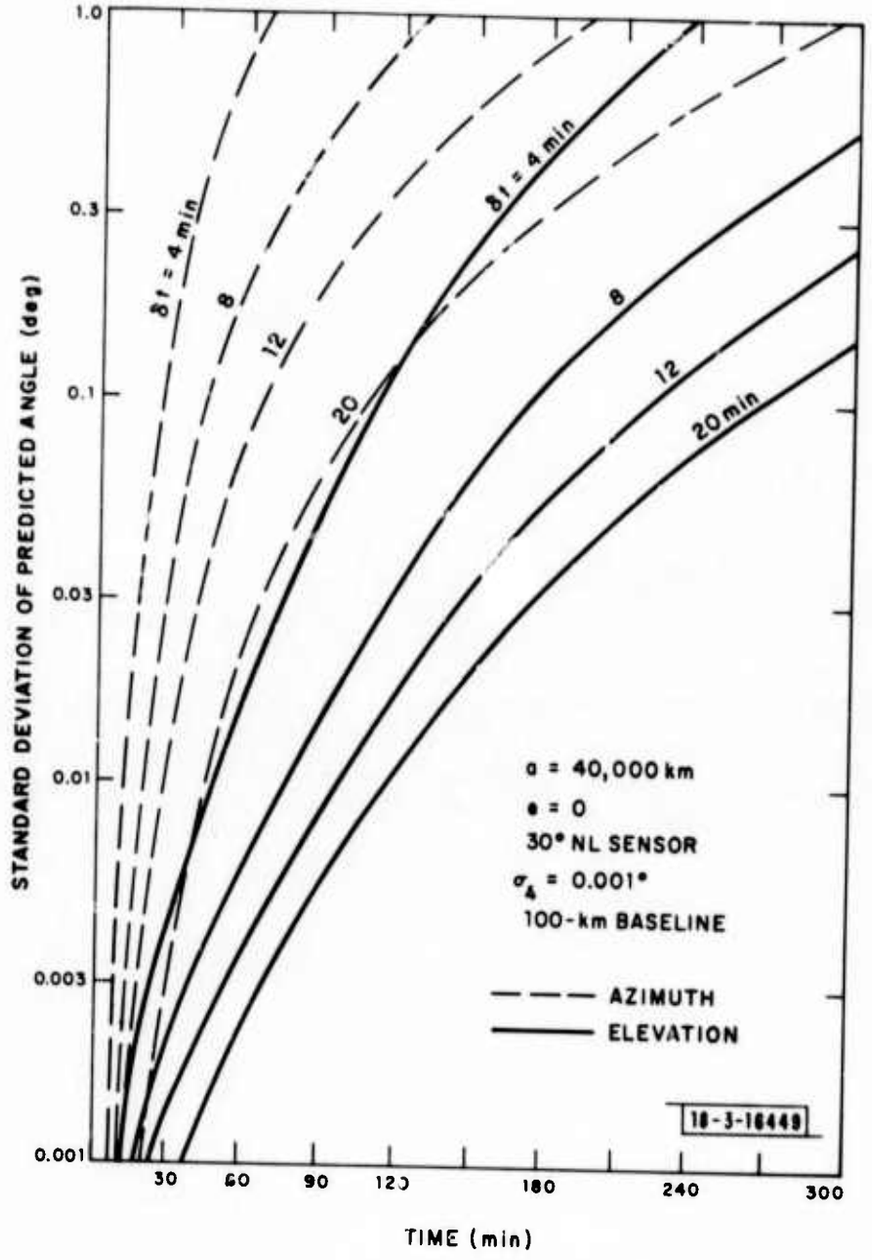

Fig. IV-3. Dual Sensor, 1 x Sync., Short Extrapolation

TABLE IV-1

SHORT-TERM EXTRAPOLATION SUMMARY

1 x Sync. Orbit

Single Sensor

Obs. Interval δt (min.)	Time $\sigma_A = 0.2°$ (min.)	Time $\sigma_A = 1°$ (min.)
4	24	45
8	45	78
12	60	112
20	90	150

Dual Sensor

Obs. Interval δt (min.)	Time $\sigma_A = 0.2°$ (min.)	Time $\sigma_A = 1°$ (min.)
4	30	66
8	60	130
12	90	195
20	147	294

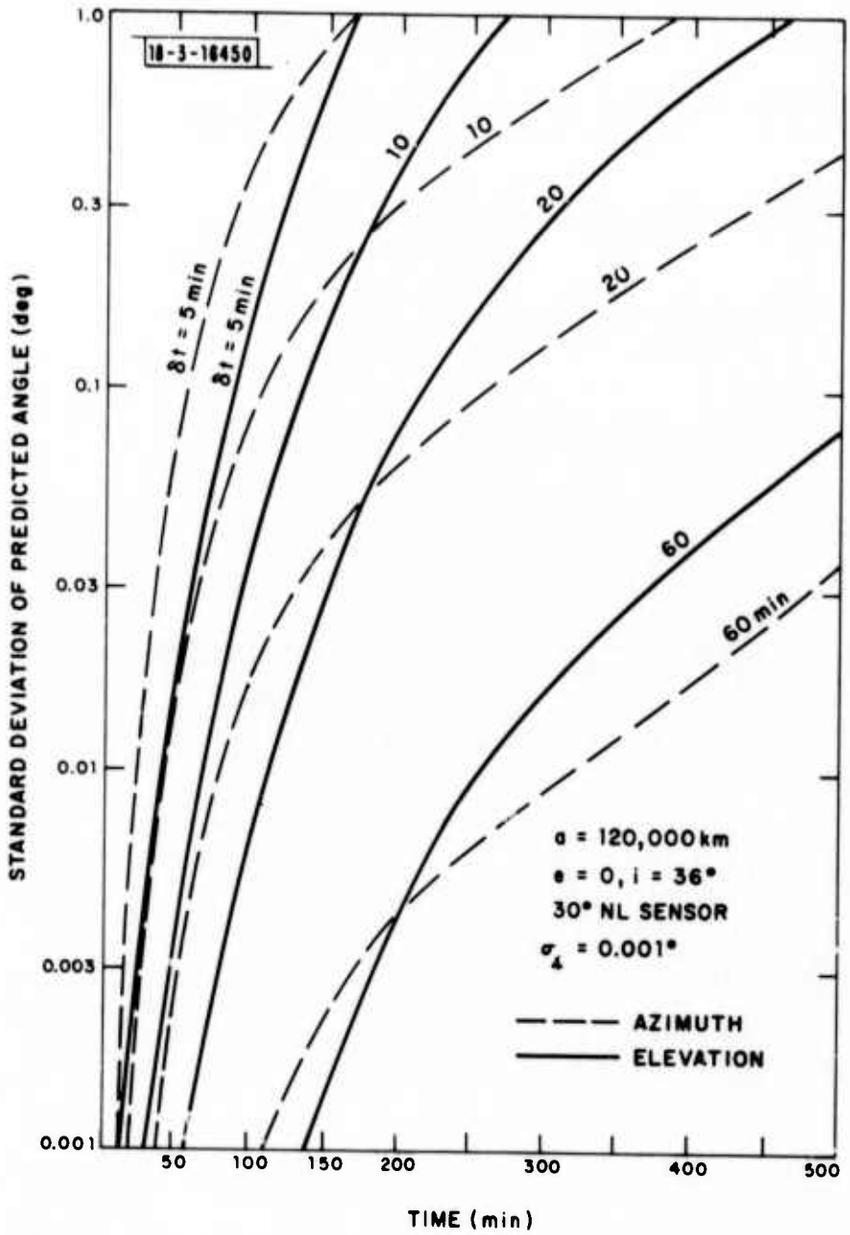

Fig. IV-4. Single Sensor, 3 x Sync., Short Extrapolation

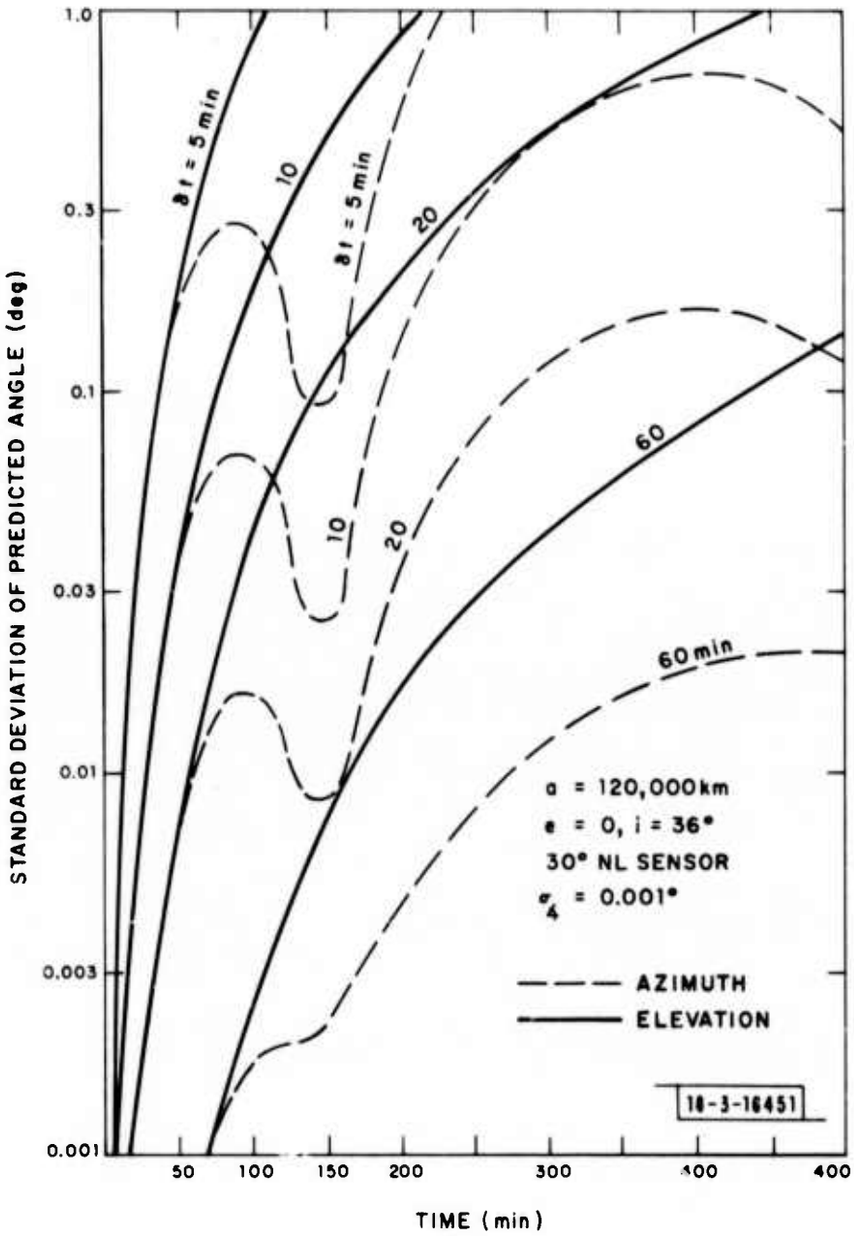

Fig. IV-5. Dual Sensor, 3 x Sync., Short Extrapolation

TABLE IV-2

SHORT-TERM EXTRAPOLATION SUMMARY

3 x Sync. Orbit

Single Sensor

Obs. Interval δ_t (min.)	Time $\sigma_A = 0.2°$ (min.)	Time $\sigma_A = 1°$ (min.)
5	32	57
10	56	109
20	105	260
60	320	~700

Dual Sensor

Obs. Interval δ_t (min.)	Time $\sigma_A = 0.2°$ (min.)	Time $\sigma_A = 1°$ (min.)
5	55	110
10	110	220
20	210	450
60	~550	--

B. Long-Term Observations

Again, the 1 x synchronous altitude orbit is considered first. It is evident from Table IV-1 that short-term extrapolation times on the order of 30 - 140 minutes are reasonable. Thus, for purposes of illustrating the effects of the time between observation intervals, ΔT, and the number of intervals, n, on the long-term extrapolation errors, the choices of ΔT = 40, 70, 100, and 135 were made. Various numbers of observation intervals were used and are indicated in the results. Figs. IV-6 to 9 illustrate the standard deviation of error in angle versus extrapolation time. Table IV-3 provides the angular errors in azimuth and elevation after extrapolation for one orbit period ($\approx$24 hours). It is interesting to note that the number of observation intervals is not so important, but rather the total time span over which measurement data was accumulated. This is evidenced by the similarity of the resulting error volume in the last box in each row. These "last box" results differ in number of observation intervals, but the total time span of measurements in each case is from 350 to 405 minutes.

The 3 x synchronous altitude orbit short-term results from Table IV-2 indicate time on the order of 30 to 200 minutes are feasible. Thus, the times of ΔT = 30, 60, 120, 180 minutes were chosen to illustrate results. Figs. IV-10 to 13 plot the standard deviation of error in angle versus extrapolation time with the number of observation intervals as a parameter. The dip in elevation prediction error occurring at 7000 minutes in these figures is believed to result from the orientation of the elongated three dimensional error ellipsoid relative to the direction of increasing elevation. Tables IV-4 and 5 summarize the results for extrapolation times of 24 hours and one orbit period ($\approx$5 days). Again the similarity of errors is evident when the total time span over which data is accumulated is the same.

In both the 1 x synchronous and 3 x synchronous altitude cases it is clear that the errors are not exceedingly large after 24 hours of extrapolation if the total observation time span is approximately 400 minutes.

C. Conclusions

As evidenced by the short-term results significant extrapolation times are feasible using reasonable observation intervals. For the 1 x synchronous orbit both the single-and dual-sensor systems yielded similar

extrapolation results. The benefits of the dual sensor were clearly indicated for the 3 x synchronous orbit by increased extrapolation times. More cases must be studied before a general conclusion can be drawn, but the dual sensor shows definite possibilities.

For the long-term extrapolation results the difference between single and dual sensor is negligible. It is evident that the most important factor is the total time span over which observations were taken. This fact is illustrated for both the 1 and 3 x synchronous orbits. It is clear that the optical systems presented are capable of developing a good ephemeris and are able to recognize the satellite on the next occasion that it becomes visible to that sensor by extrapolation of the developed ephemeris.

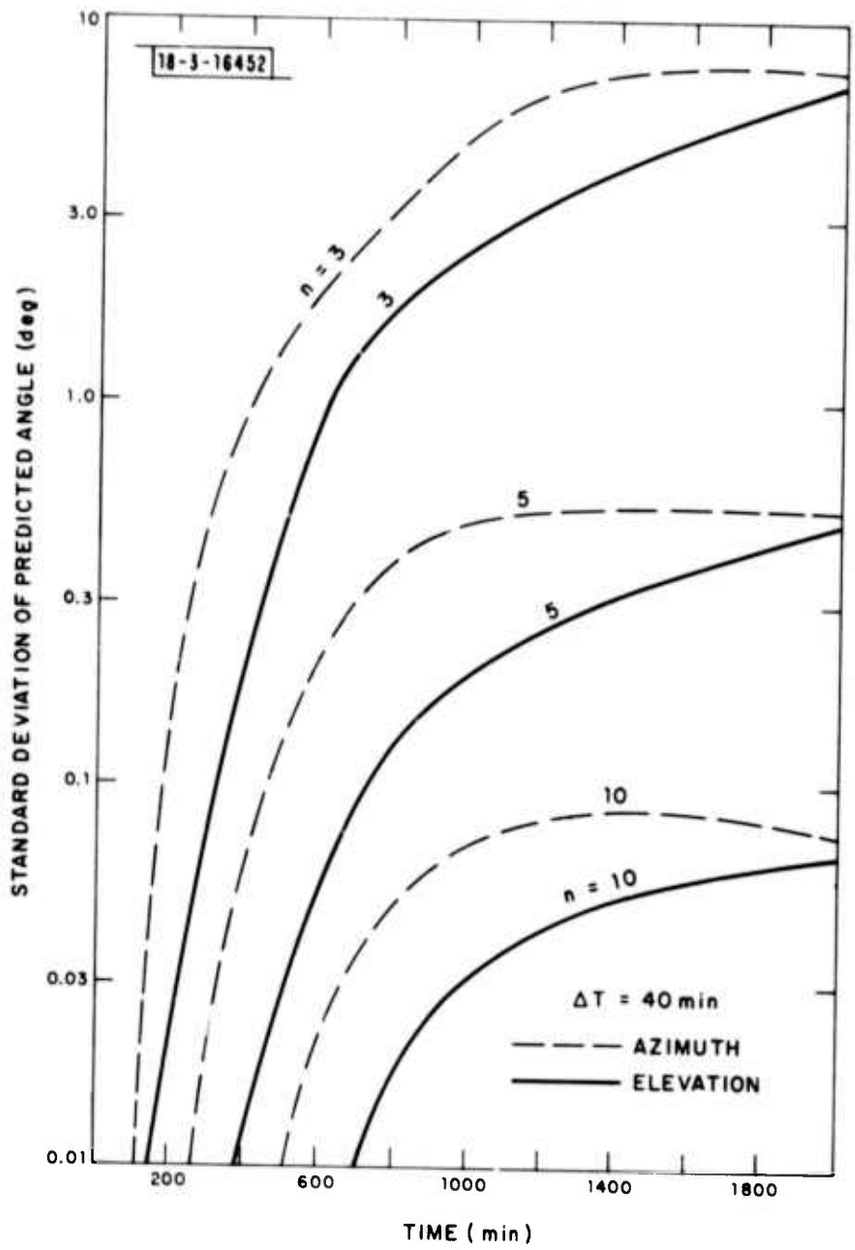

Fig. IV-6. Long Extrapolation, 1 x Sync., Δt = 40 min.

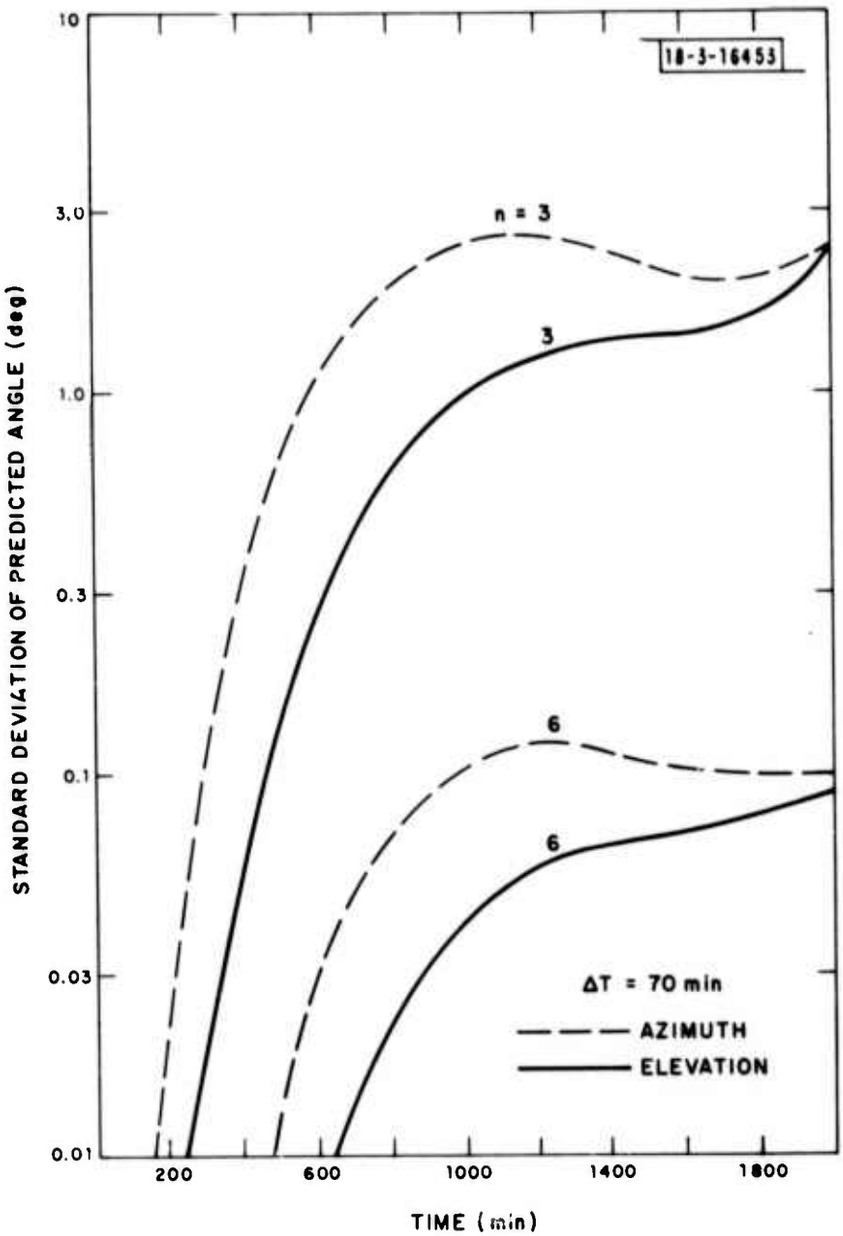

Fig. IV-7. Long Extrapolation, 1 x Sync., Δt = 70 min.

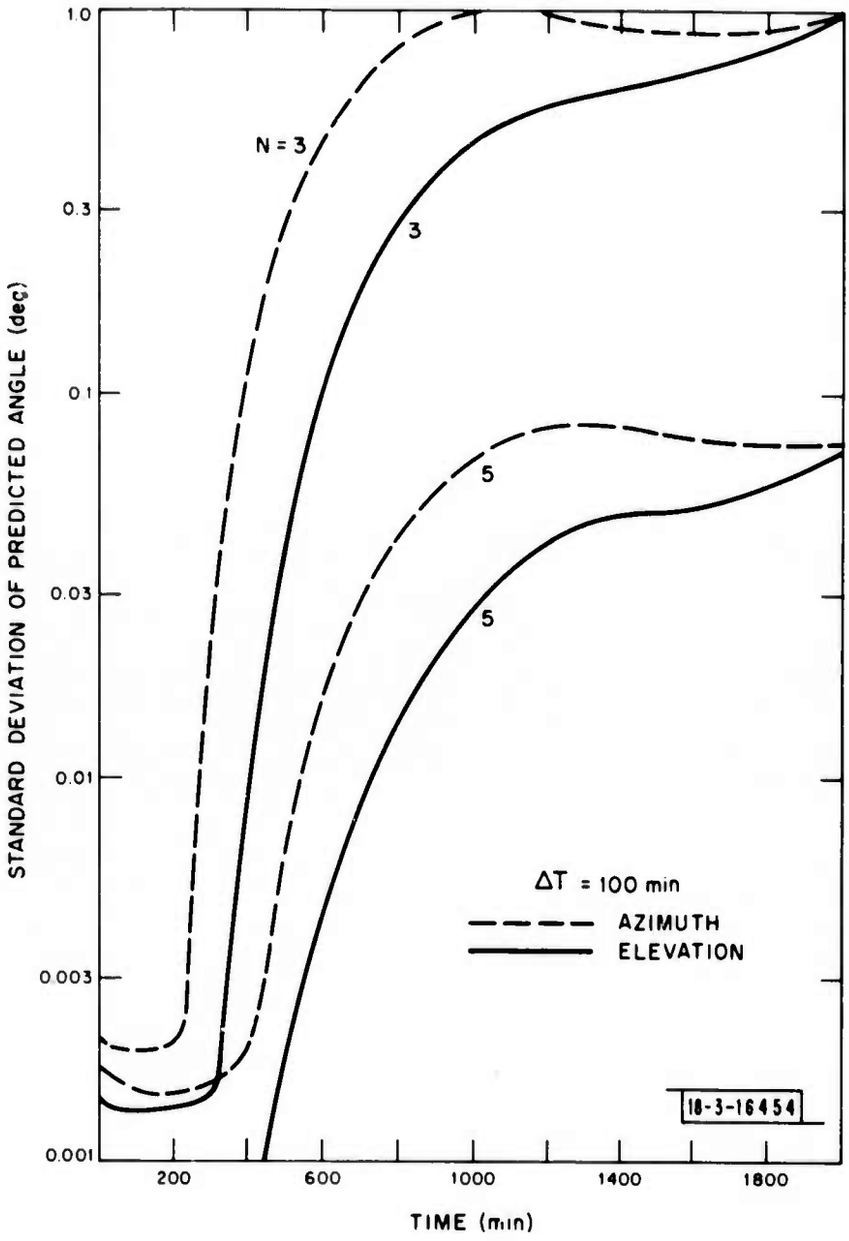

Fig. IV-8. Long Extrapolation, 1 x Sync., Δt = 100 min.

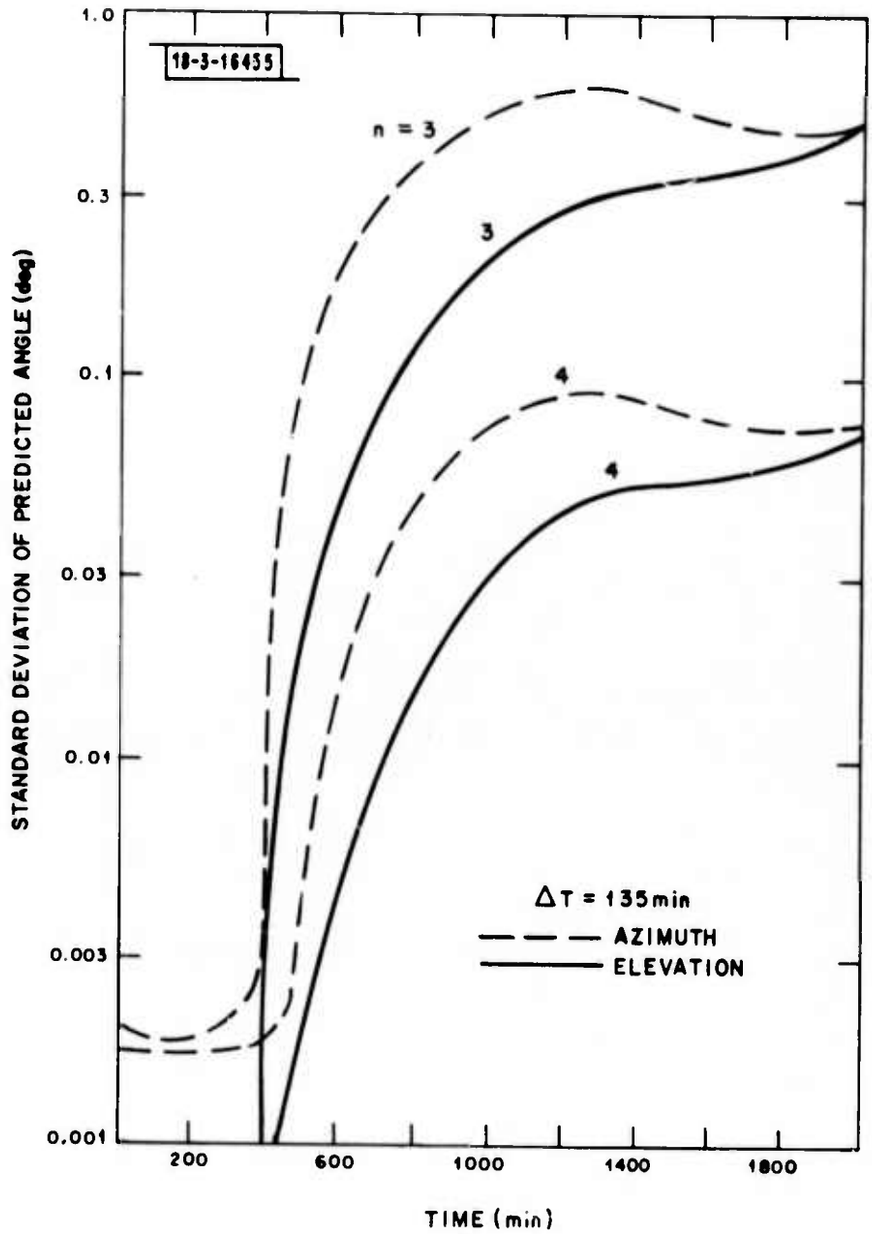

Fig. IV-9. Long Extrapolation, 1 x Sync., Δt = 135 min.

TABLE IV-3

LONG-TERM EXTRAPOLATION SUMMARY

1 x Sync. Orbit

(Standard Deviation of Predicted Angular Error in Degrees after Extrapolation for One Orbital Period)

Time Interval ΔT (min.)	Number of Data Sets, N				
	3	4	5	6	10
40	7.2/4.2**		0.55/0.33		0.09/0.05
70	2.2/1.3			0.1/0.07	
100	1.1/0.63		0.08/0.05		
135	0.6/0.33	0.09/0.05			

** Azimuth Angle/Elevation Angle

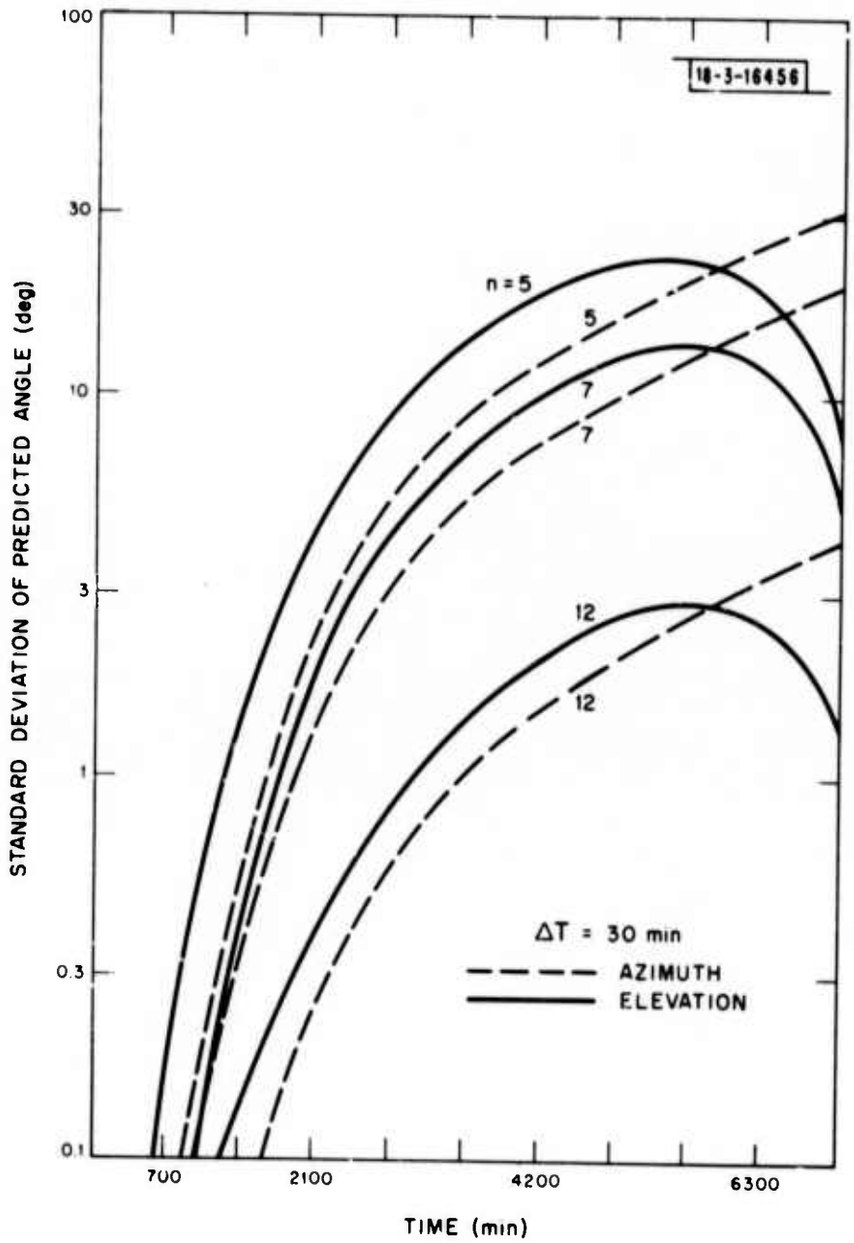

Fig. IV-10. Long Extrapolation, 3 x Sync., Δt = 30 min.

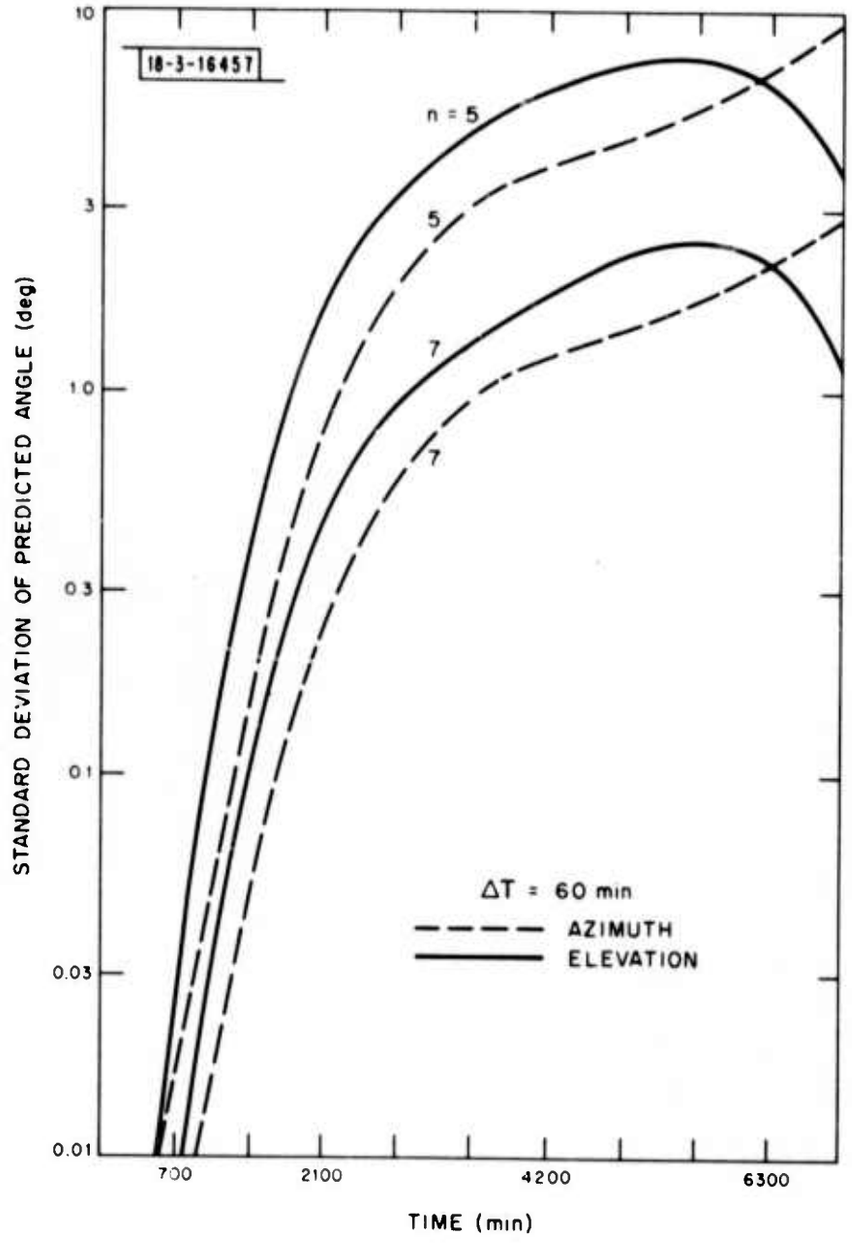

Fig. IV-11. Long Extrapolation, 3 x Sync., Δt = 60 min.

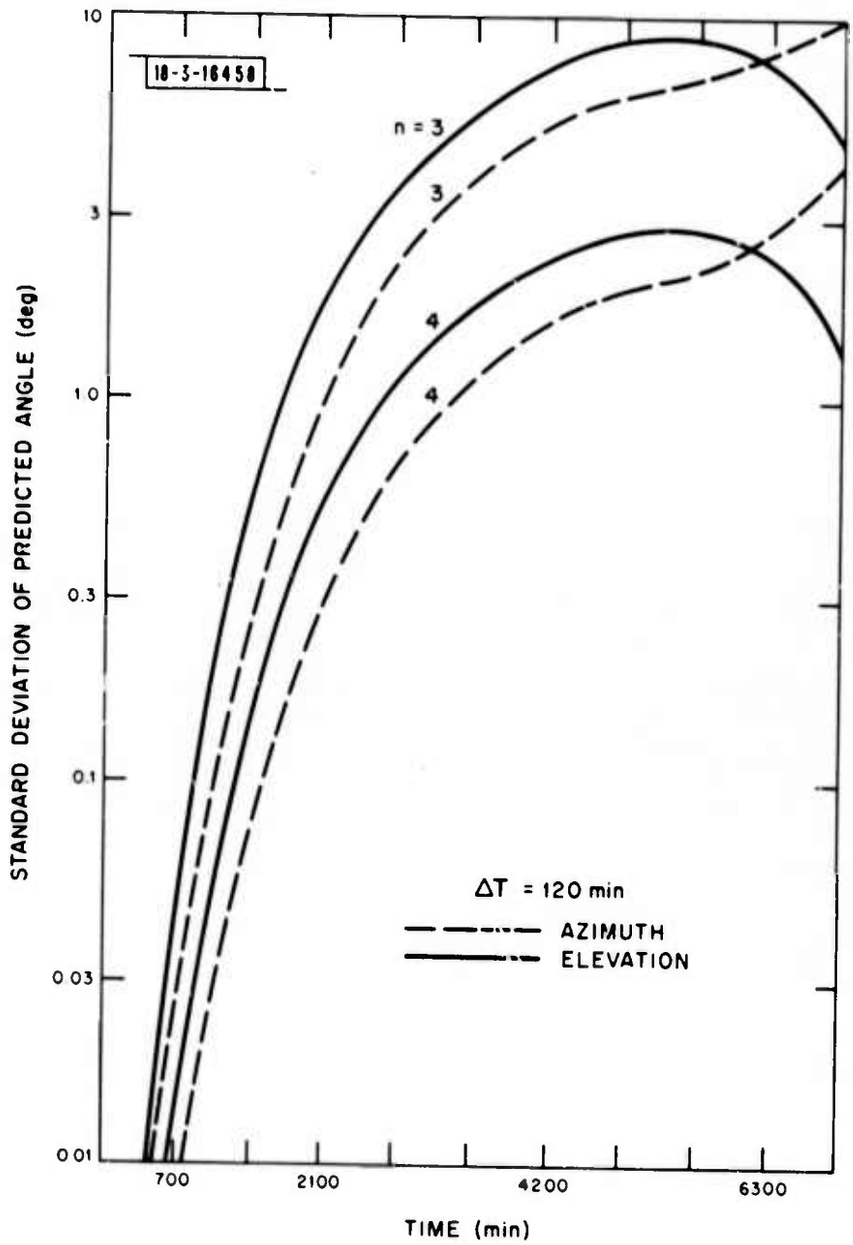

Fig. IV-12. Long Extrapolation, 3 x Sync., Δt = 120 min.

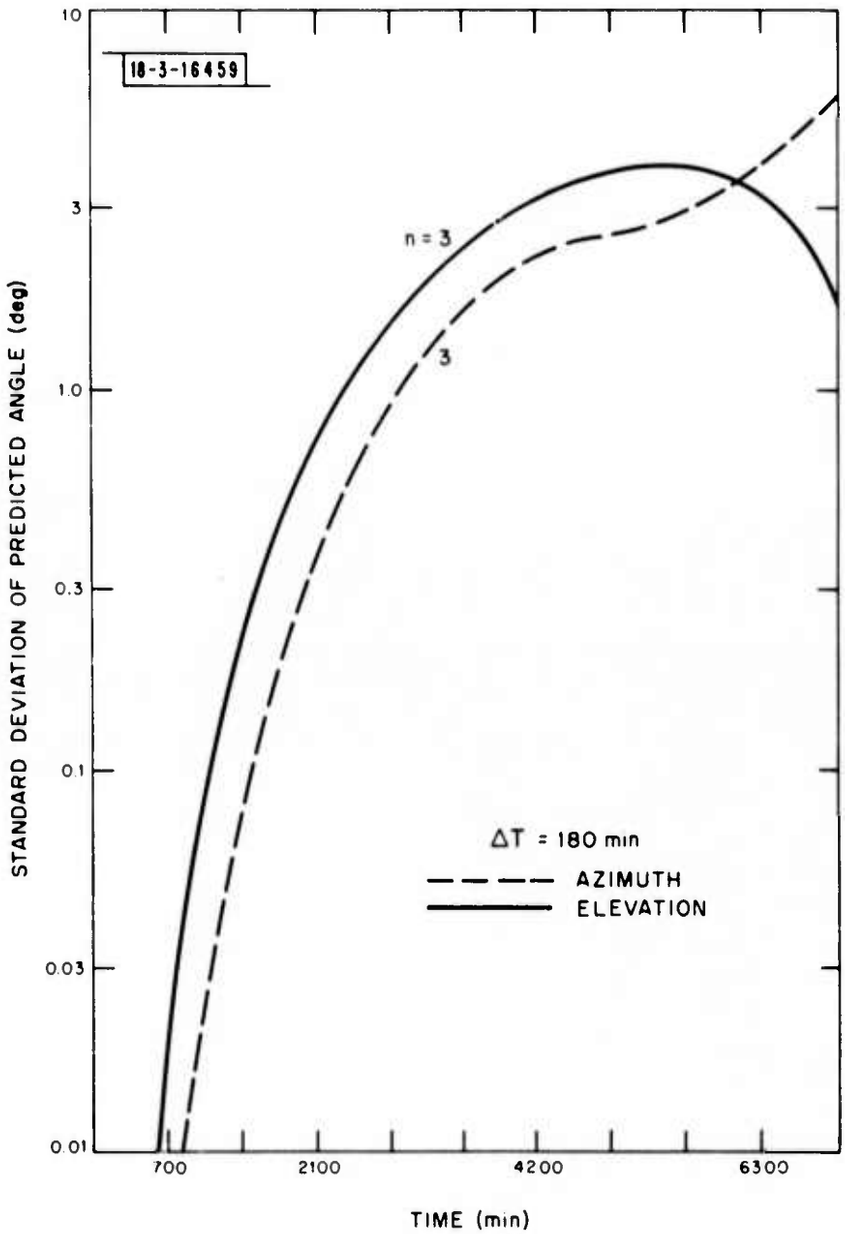

Fig. IV-13. Long Extrapolation, 3 x Sync., Δt = 180 min.

TABLE IV-4

LONG-TERM EXTRAPOLATION SUMMARY

3 x Sync. Orbit

(Standard Deviation of Predicted Angular Error in Degrees after Extrapolation for 24 hours)

Time Interval ΔT (min.)	Number of Data Sets, N				
	3	4	5	7	12
30			* 0.7/1.6	0.4/0.9	0.07/0.16
60			0.2/0.5	0.06/0.15	
120	0.25/0.6	0.07/0.17			
180	0.08/0.19				

* Azimuth Angle/Elevation Angle

TABLE IV-5

LONG-TERM EXTRAPOLATION SUMMARY

3 x Sync. Orbit

(Standard Deviation of Predicted Angular Error in Degrees after Extrapolation for One Orbit Period)

Time Interval ΔT (min.)	Number of Data Sets, N				
	3	4	5	7	12
30			* 65/27	40/16	6.5/3.5
60			25/10	8.2/3.3	
120	23/12	9.6/3.9			
180	10.9/4.4				

* Azimuth Angle/Elevation Angle

V. GROUND-BASED-RADAR ERROR ANALYSIS

A. General

Computer simulation studies were run to evaluate the effects on target reacquisition for various observation intervals and extrapolation times up to 10 days. In each case the sensor was allowed to make observations of the target and the orbital parameters were extrapolated for 10 days. An error analysis propagated the covariance matrix along the trajectory. This covariance matrix determines the error volume about the nominal trajectory. The results of the error analyses are presented in the sensor's coordinate system (i.e., range, azimuth, elevation, range-rate).

B. RADAR 1, Track Data Rate Algorithm

A track data rate algorithm was chosen which used approximately 10% of the surveillance energy. The radar beam must dwell approximately 1.2 seconds in each position to develop the required 10 dB S/N. Therefore, once a detection is made, the radar beam will return to that beam position in 12 seconds for another look. If the satellite was at an altitude slightly less than synchronous altitude its angular velocity relative to the earth could be approximately .05°/min, however, a satellite in a highly elliptical orbit with apogee near synchronous altitude would have an angular velocity near apogee of 0.18°/min. A satellite with an angular velocity of 0.2°/minute will move 0.04 degree in 12 seconds. The radar has a very high probability of seeing the satellite to obtain a second data point. This high data rate interval (1 observation every 12 seconds) is arbitrarily set at 1 hour. After the first hour of observation the data rate is reduced to 1 observation every 5 minutes. At each observation point, 10 track data pulses are noncoherently averaged to improve the S/N and hence reduce the measurement uncertainty. The second data interval is allowed to vary and the results are compared in the analyses that follow. This algorithm, most likely, is more than sufficient to do the job. It is not the purpose of this note to optimize the use of radar resources. There is no doubt that a more efficient algorithm could be designed which would conserve radar and computer resources.

The measurement uncertainties have been shown* to vary according to the following relationship.

$$\sigma = \frac{\text{resolution}}{\sqrt{n\ S/N}}$$

Where n = number of pulses

Detection is assumed to occur as the satellite enters the field of view. The radar was arbitrarily placed at 30° N, 160° W with the satellite starting at 170° E. At this point the radar beam from the phased array has broadened from its nominal value at boresite. Consequently, the measurement uncertainty in angle will be increased by a proportionate amount. The measurement uncertainties used in the error analyses are contained in Table V-1.

TABLE V-1

MEASUREMENT UNCERTAINTIES

Coordinate	σ
R	$\delta r/3 = 10,000$ km
$\measuredangle$	$\delta\measuredangle/2 = .5^{\circ}$
$\dot{R}$	$\delta\dot{r}/3 = .35$ m/sec

The observation intervals used in the error analysis for the 1 x sync. orbit are listed in Table V-2.

* R. Manasse, "Summary of Maximum Theoretical Accuracy of Radar Measurements", Mitre Corporation, Technical Series Report No. 2 (April 1, 1960).

TABLE V-2

OBSERVATION INTERVALS (1 x Sync. Orbit)

Case Number	Date Rate	Data Interval
1	1 obs/12 sec	1 Hr
2	1 obs/12 sec	1 Hr
	1 obs/5 min	1 Hr
3	1 obs/12 sec	1 Hr
	1 obs/5 min	2 Hr
4	1 obs/12 sec	1 Hr
	1 obs/5 min	4 Hr
5	1 obs/12 sec	1 Hr
	1 obs/5 min	8 Hr
6	1 obs/12 sec	1 Hr
	1 obs/5 min	16 Hr
7	1 obs/12 sec	1 Hr
	1 obs/5 min	4 Hr
	1 obs/5 min (1 period later)	1 Hr

C. Error Analysis (1 x Sync Orbit; RADAR 1)

Figure V-1 shows the growth of the error ellipsoid in terms of radar angular coordinates (azimuth and elevation) for the initial data rate and observation interval. In order to have greater than 99% probability of having the target within one beamwidth, the radar must return for additional track data within 40 minutes. Reacquisition at the edge of the beam would mean a possible reduction of 3 dB in signal strength and a large increase in the number of false alarms. A more tolerable loss in signal strength would be 1 dB. This occurs after 5 minutes of extrapolation. This appears to be a more reasonable degradation in signal strength for maintaining "good" track.

Figures V-2, 3, 4, 5 show the growth of the error ellipsoid in the four radar coordinates, range, azimuth, elevation and range-rate, respectively, as a function of time. The sharp minima which occur in Figs. V-2, 4 and 5 are believed to result from the orientation of the 3-dimensional error ellipsoid relative to the radar polar coordinates. Table V-3 summarizes these

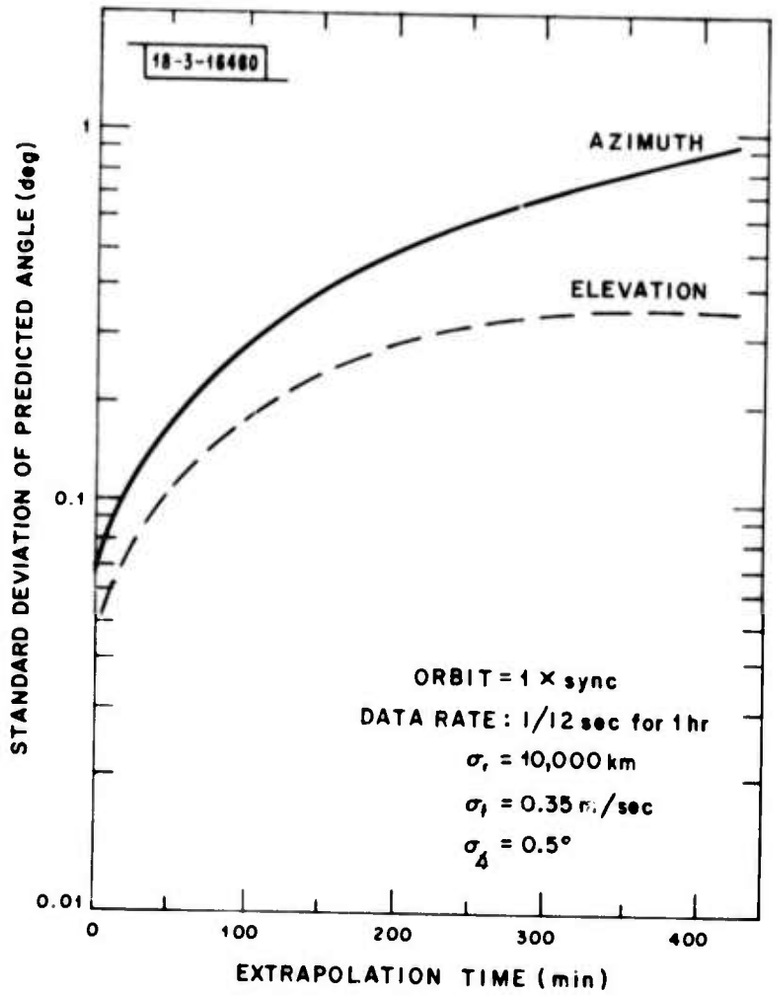

Fig. V-1. RADAR 1 Angle Errors vs. Time

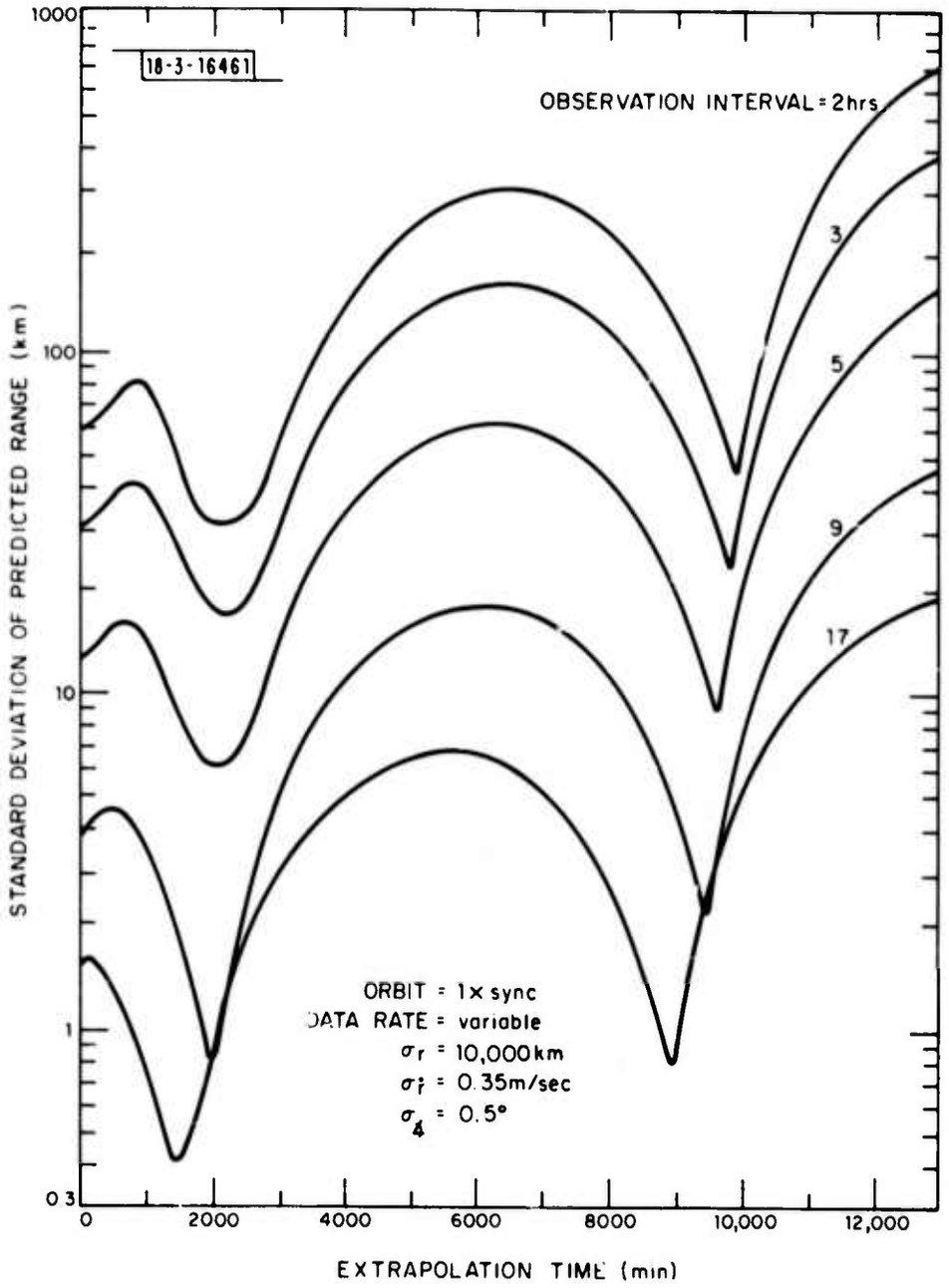

Fig. V-2. RADAR 1 Range Errors vs. Time

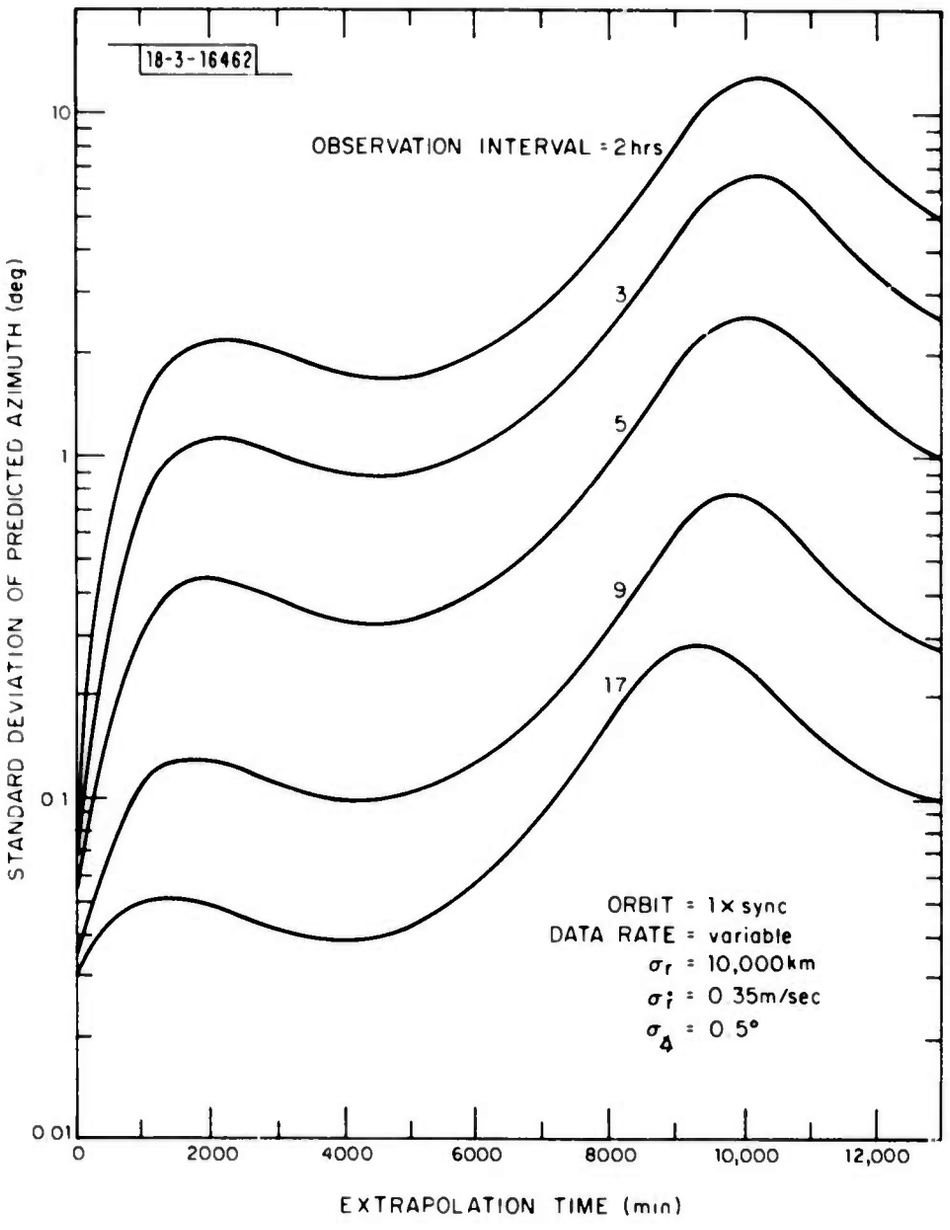

Fig. V-3. RADAR 1 Azimuth Errors vs. Time

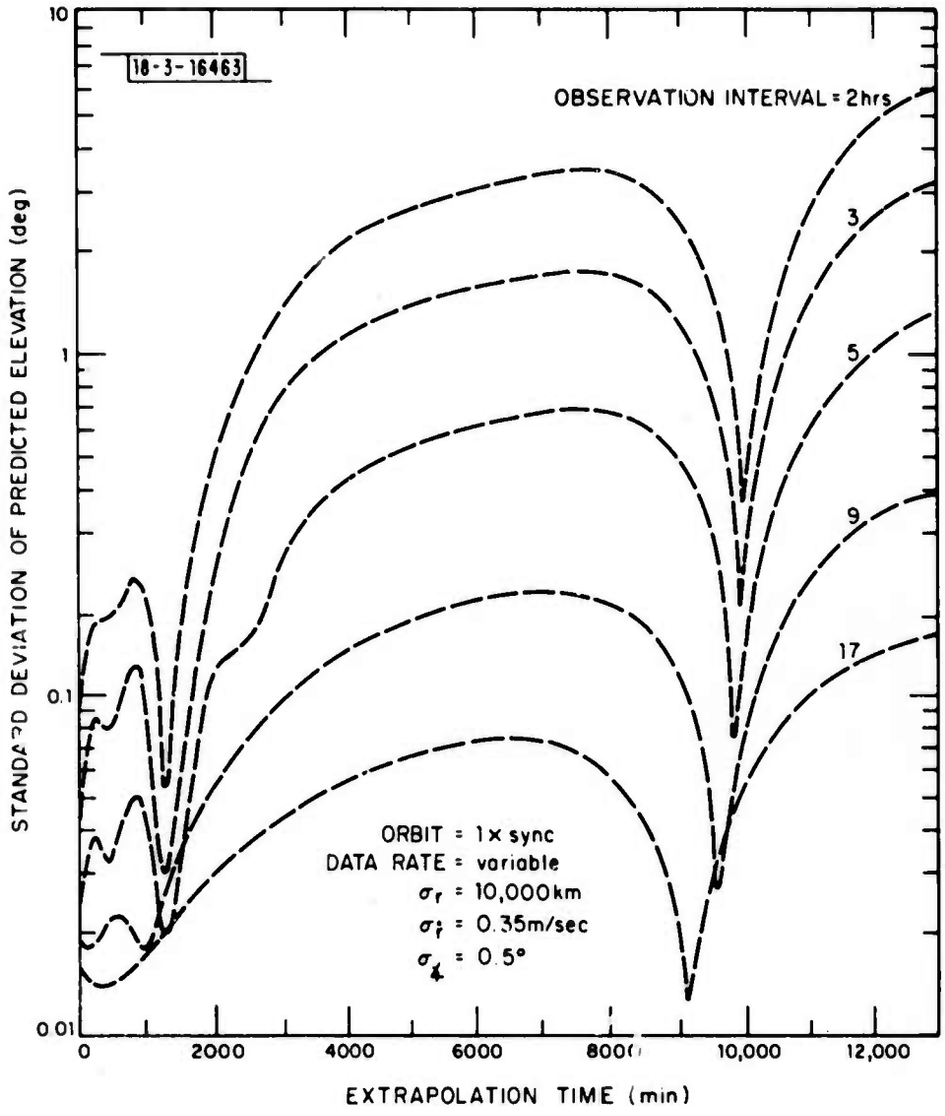

Fig. V-4. RADAR 1 Elevation Errors vs. Time

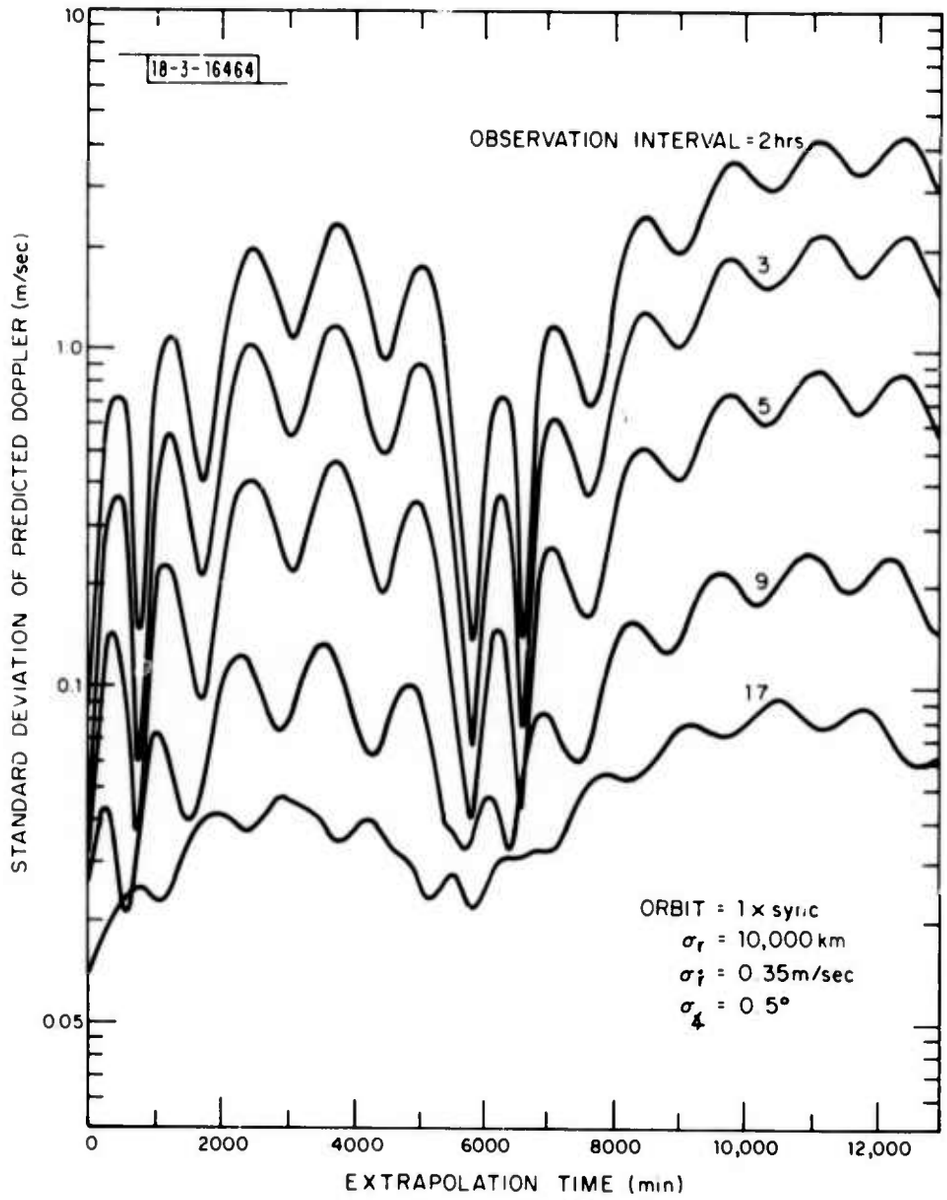

Fig. V-5. RADAR 1 Doppler Errors vs. Time

TABLE V-3

1 σ ERROR vs. TIME*

Observation Interval	Time	σ_r(Km)	σ_{Az}(Deg)	σ_{El}(Deg)	$\sigma_{\dot{r}}$(m/s)
2 Hrs.	EOT	60	.08	.05	.04
"	1 Day	81	1.8	.25	1.1
"	10 Day	930	13	7.3	4.0
3 Hrs.	EOT	31	.06	.04	.04
"	1 Day	41	.9	.12	.56
"	10 Day	480	7	3.8	2.1
5 Hrs.	EOT	12	.05	.03	.03
"	1 Day	16	.35	.05	.23
"	10 Day	190	2.6	1.5	1.1
9 Hrs.	EOT	3.6	.03	.02	.03
"	1 Day	4.6	.10	.02	.07
"	10 Day	55	.76	.43	.86
17 Hrs.	EOT	1.6	.03	.02	.01
"	1 Day	1.6	.04	.02	.02
"	10 Day	20	.28	.16	.26

*1 x Sync Orbit

Radar 1

Maximum value during the extrapolation period is indicated

results and lists the 1 σ error at the end of track (EOT), maximum value during the first day (1 Day) and maximum value during ten days (10 Days).*

The angular errors after 9 hours of observation show that the trajectory could be extrapolated for 10 days and the radar would have a greater than 68% probability (± 1 σ) of being within one beam position of the target. If a greater than 99% probability (± 3 σ) of finding the target is required, the radar must search a maximum of 15 beam positions. Table V-4 lists the number of beam positions that must be searched and the search time to obtain a greater than 99% probability of finding the satellite after 10 days as a function of observation time.

TABLE V-4

SEARCH AREA AFTER 10 DAYS vs.
OBSERVATION INTERVAL (FOR 99% PROBABILITY)

Observation Interval (Hrs.)	Beam Positions	Search Time
2	~3400	71 min
3	~ 970	21 min
5	~ 140	3 min
9	15	19 sec
17	2	2.5 sec

It is apparent from Table V-4 that increasing the observation interval by a small amount reduces the required search time by a significant amount. Satellites in near synchronous orbit will remain within the sensors field of view for a long time (~ 12 - 24 hours). For example, if 10% of the time when the satellite was in the field of view of the sensor could be devoted to the reacquisition-search part of the radar task, an observation interval of 2 hours would be required. The system designer can trade observation interval for search time based on such factors as radar resources available for reacquisition-search, length of time the satellite remains in the field of view of the sensor, and the growth rate of the error volume.

* Some of the values of $\sigma_{\dot{r}}$ in Table V-3 are so small as to be of questionable credibility. The sensitivity to $\sigma_{\dot{r}}$ is explored below.

The angular errors are much smaller after extrapolating the trajectory for 1 day rather than the 10-day interval considered above. Let us assume that the radar will be allowed to observe the satellite initially for 5 hours. After extrapolating for 1 day, the radar will reacquire the target and track for an additional 1 hour at a data rate of one observation every 5 minutes. Fig. V-6 compares the standard deviation in angle over a 10-day interval for an observation interval of 5 hours and an observation interval of 5 hours plus 1 hour 1 orbital period later. The errors are reduced almost an order of magnitude when the additional 1 hour of observations 1 orbital period later is included in the data base. The maximum standard deviation during a 10-day period is 0.35 degrees in azimuth and 0.17 degrees in elevation. The additional 1-hour observation interval 1 orbital period later produces errors similar to those resulting from an initial 17-hour observation interval. A considerable amount of observation time can be saved using this method of orbit determination and refinement.

The radar waveforms were designed with an option to improve the range resolution. A 10-KC bandwidth pulse was postulated which results in a 15-km range resolution. The effect of improved range resolution on the angular prediction errors was investigated. In addition, the effect of using the CW pulse and poor Doppler resolution on the angle errors was studied. Fig. V-7 shows the improvement in angle error using a pulse with 15 km range resolution. The reduction in the standard deviation of the azimuth error is about 2 to 5 times. There is a much smaller reduction in the elevation error. Fig. V-8 shows the degradation in angle error as Doppler information is denied in the error analysis. Table V-5 lists the maximum standard deviation in angle during 24 hours of extrapolation time for the CW and coded waveforms. The range-rate resolution was varied between the best possible and no range-rate information. In general the angle errors will be within a tolerable error if the radar is denied either accurate range or range-rate data. If the radar is denied both, the errors become extremely large using angle only information.

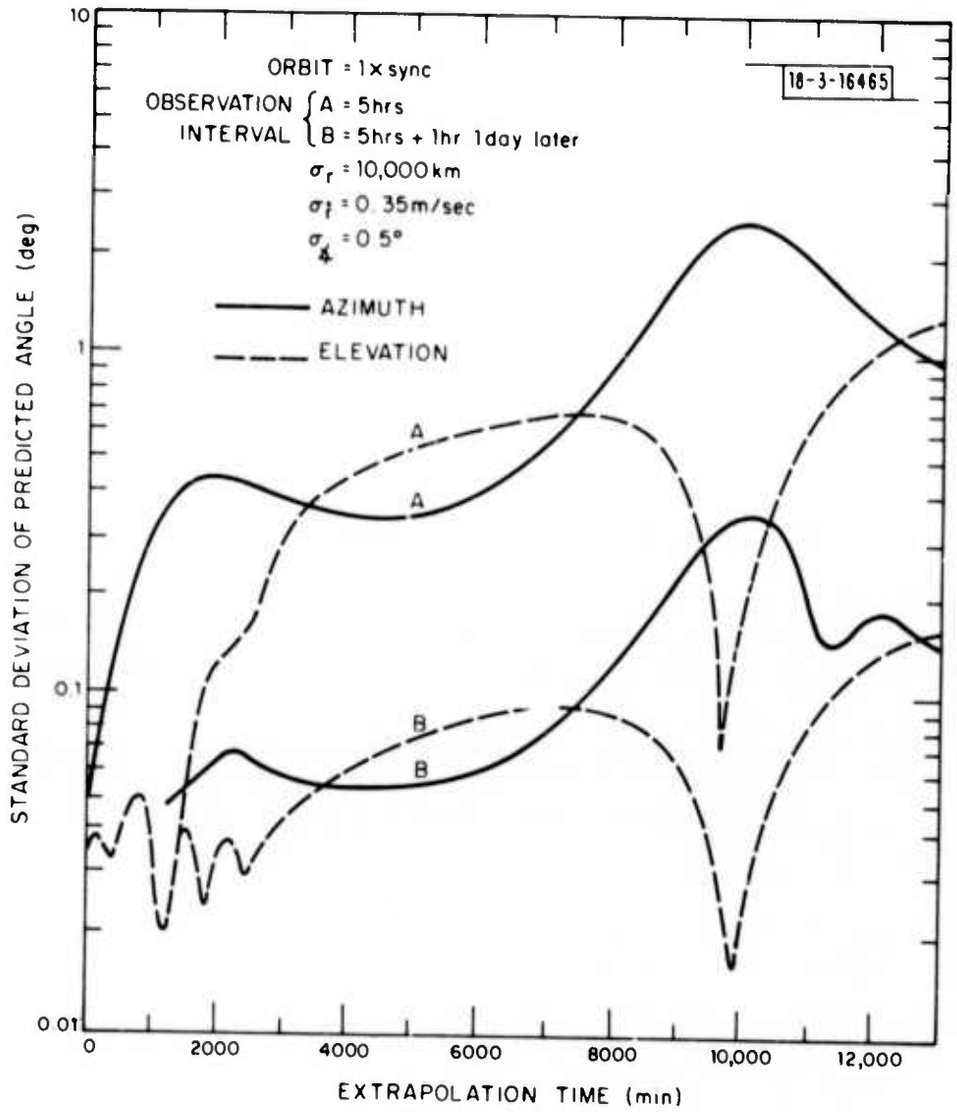

Fig. V-6. RADAR 1 Angle Errors vs. Time

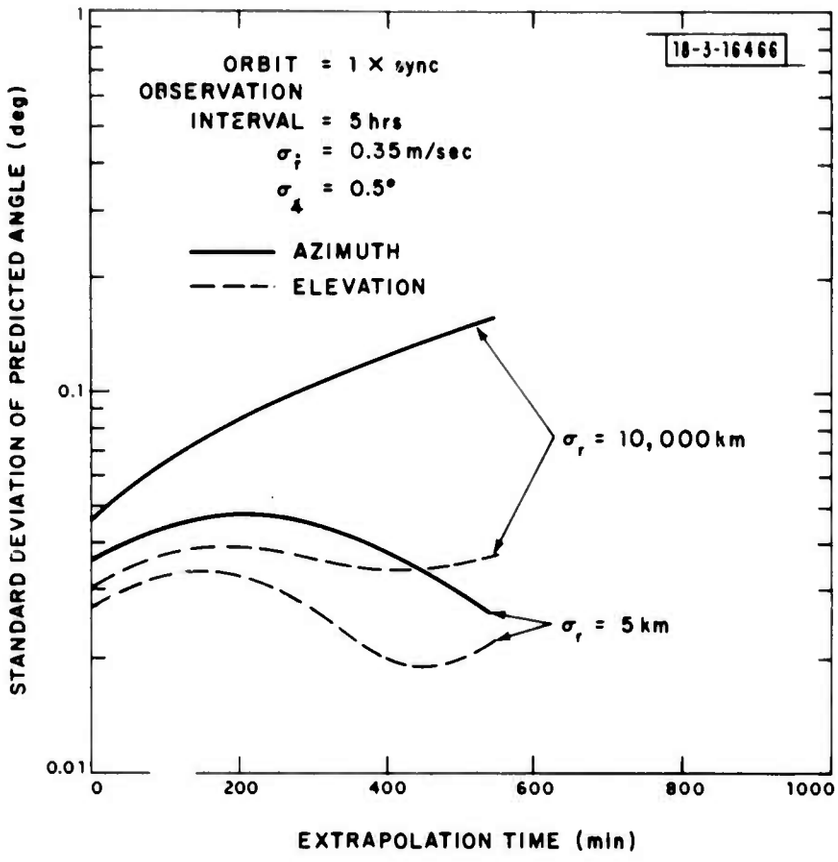

Fig. V-7. RADAR 1 Angle Errors vs. Time

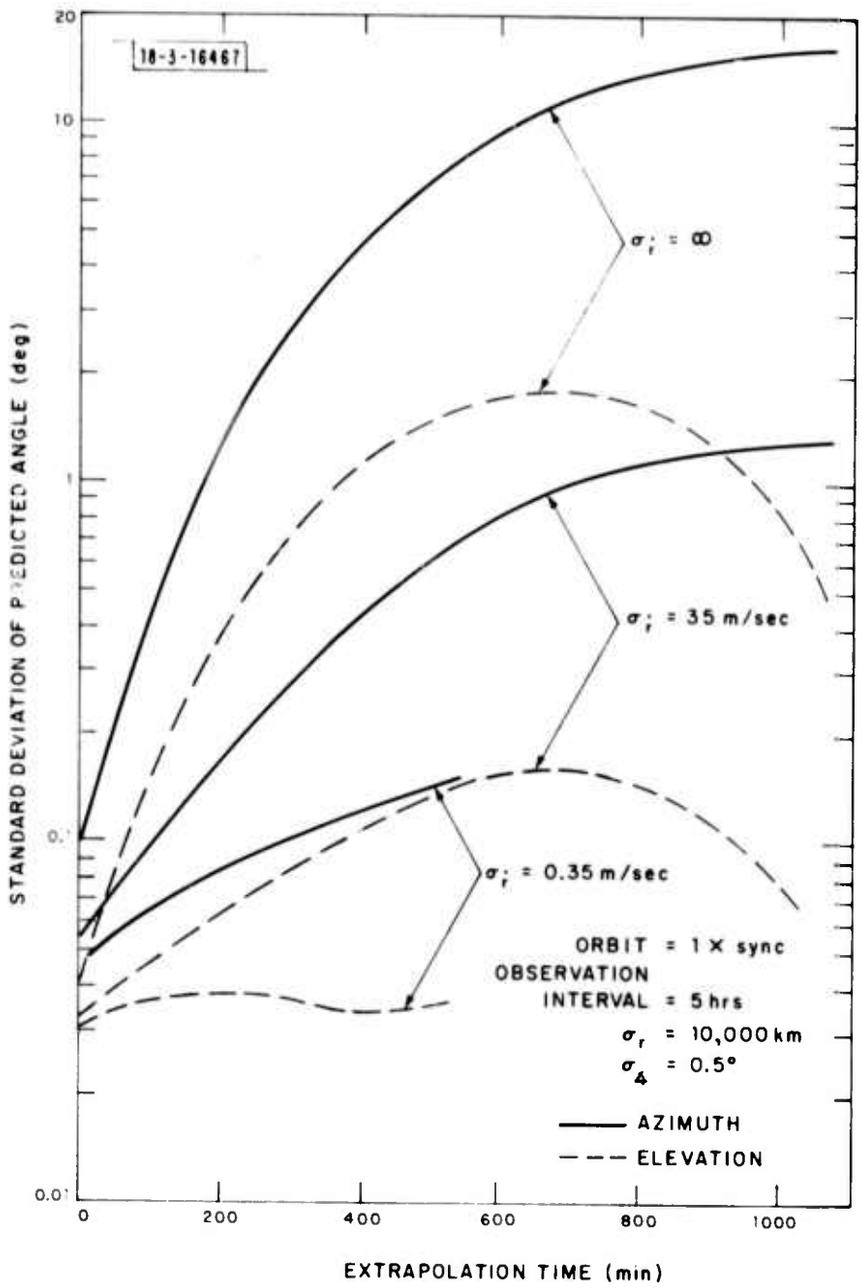

Fig. V-8. RADAR 1 Angle Errors vs. Time

TABLE V-5

ERRORS IN PREDICTED ANGLES vs. RANGE AND DOPPLER ERRORS

Observation Std. Dev. Range (km)	Range-Rate (m/s)	Std. Dev. Predicted Angle Error (deg)
10,000	0.35	< 0.20
10,000	35	< 2.0
10,000	∞	< 20.0
15	0.35	< 0.05
15	∞	< 0.70

* 1 x sync. orbit

RADAR 1

Entries are max. values over 24 hours extrapolation time

Radar Resolution

Range = 30,000 km

Angle = 1.0°

Doppler = 1 m/sec

D. Error Analysis (Molniya; RADAR 1)

In this section, the growth of the angular errors resulting from a track of a typical Molniya-type orbit is studied. A track data rate algorithm similar to the one used in the previous section will be used. The satellite orbital period is one-half that of the earth, consequently, the observation interval will be limited by the time the satellite spends in the field of view of the radar. The radar was arbitrarily placed at 35° N, 105° W. Figure V-9 shows the position of the satellite on an elevation-azimuth plane. Superimposed on the plot is the field of view of the radar. The satellite enters the field of view twice a day and remains in the field of view for 170 and 330 minutes. Observation is assumed to occur during the longer interval. This analysis uses the tracking waveform shown in Fig. II-1b with 15 km range resolution. The measurement uncertainties used in the error analysis are similar to those of the previous section, however, the effects of the R^4 variation in S/N are taken into account.

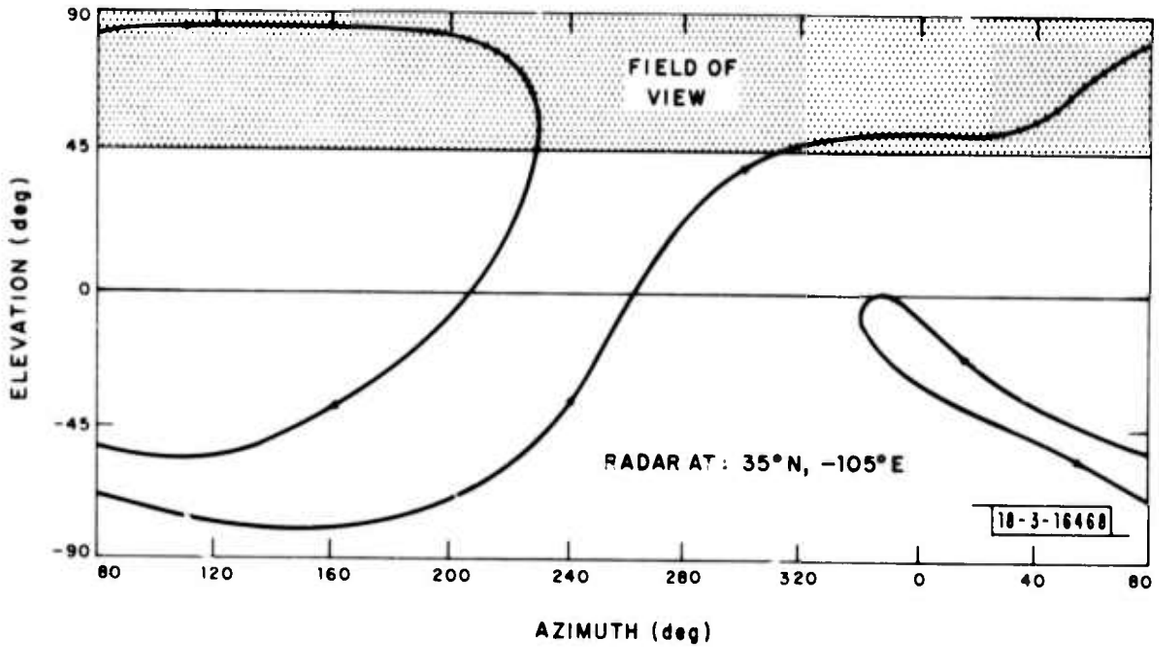

Fig. V-9. Molniya Visibility

The NRTPOD program modifies the standard deviation of the observations using

$$\sigma = \sqrt{A^2 + B^2 \frac{R^4}{f(\theta)}}$$

where A = nominal standard deviation at very large signal to noise

$f(\theta)$ = cross section as a function of aspect angle

B = sensor constant

R = range to target in earth radii

σ = standard deviation of observation at some range

The waveform of Fig. II-1b was assumed for the error analyses of a typical Molniya orbit. The standard deviation of the measurement errors at the maximum range (≈36,000 km) are shown in Table V-6. It is assumed that at very large signal to noise ratios, the measurement errors are 1/100 of the resolution capability.

TABLE V-6

MEASUREMENT UNCERTAINTIES

Coordinate	σ
R	$\delta_{r/3}$ = 5 km
$\not<$	$\delta_{\not</2}$ = .5°
$\dot{R}$	$\delta_{\dot{r}/3}$ = .35 m/sec

Given the above values and the maximum measurement errors, the sensor constant (B) can be calculated at the maximum range (≈36,000 km). The variation of the measurement standard deviations with range is plotted in Fig. V-10. Over the observation interval, the measurement standard deviations are not linear but a function of the range.

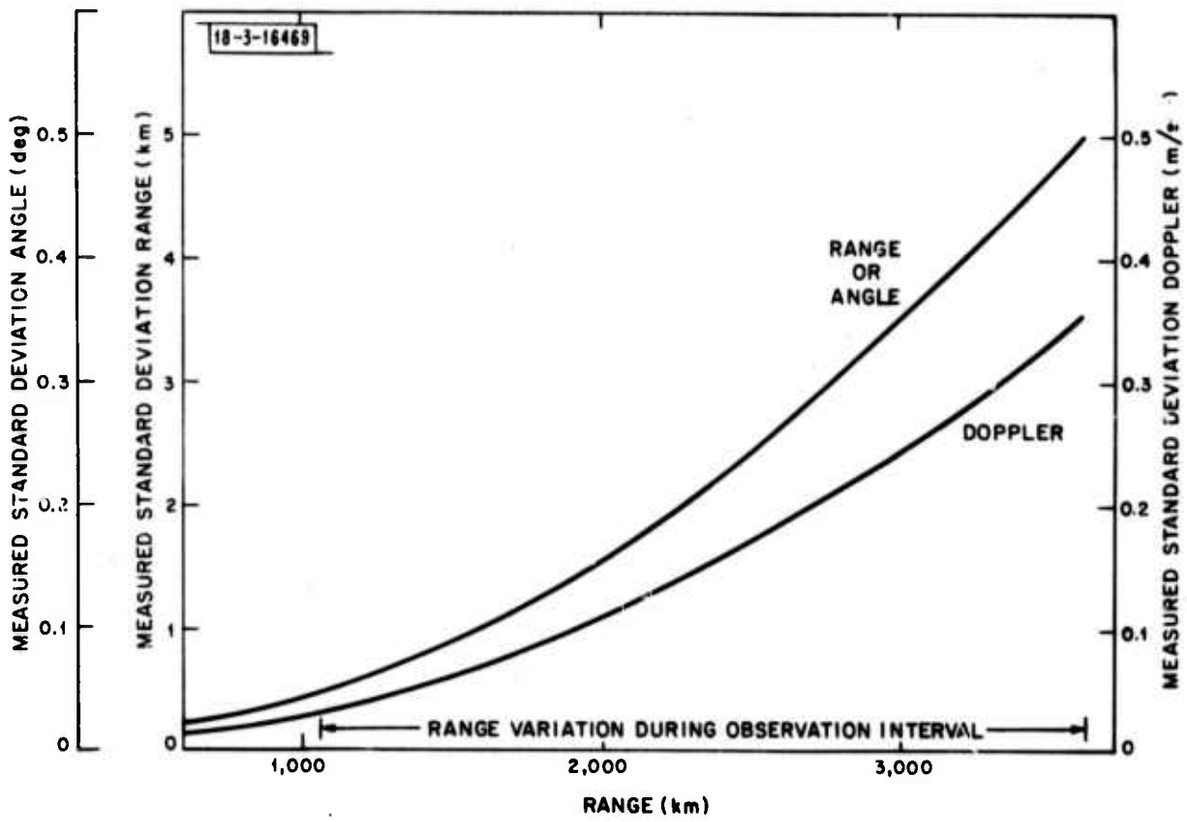

Fig. V-10. Measurement Standard Deviations vs. Range

The S/N variation during the observation interval is approximately 20 db whereas in the previous case (circular orbits) the S/N was essentially constant.

Fig. V-11 shows the variation of the standard deviation of angle errors vs. time for a 60-minute observation interval using 1 observation every 12 seconds. The extrapolated errors remain at a reasonably low value during the entire time the satellite is in the field of view of the radar. A track data rate of one observation every 5 minutes after the first hour of the observation interval is very reasonable. Fig. V-12 shows the variation of the standard deviation of angle error vs. time when the observation interval was chosen to be 165 minutes. The Doppler information was degraded in steps of 100 twice. The short-term degradation in angle errors was minimal; however, after 1 day, the angle errors begin to show a larger degradation for the poorer Doppler measurements. Table V-7 summarizes the angular errors at the end of 1 day and maximum value during 10 days.

TABLE V-7

ANGLE PREDICTION ERRORS vs. DOPPLER STD. DEV.

Time	Doppler Std. Dev.	Angle Error (deg)
1 day	0.35	0.114
10 day	0.35	2.46
1 day	35	0.240
10 day	35	4.89
1 day	3500	0.519
10 day	3500	9.93

The angle error increased by approximately a factor of 2 each time the Doppler measurement standard deviation was degraded by a factor of 100. Fig. V-13 shows the improvement obtained by using a second observation interval of 165 minutes one day later. The near-term (end of second track) improvement is approximately one order of magnitude. The improvement is two orders of magnitude after extrapolating for an additional day. Very accurate orbital data can be

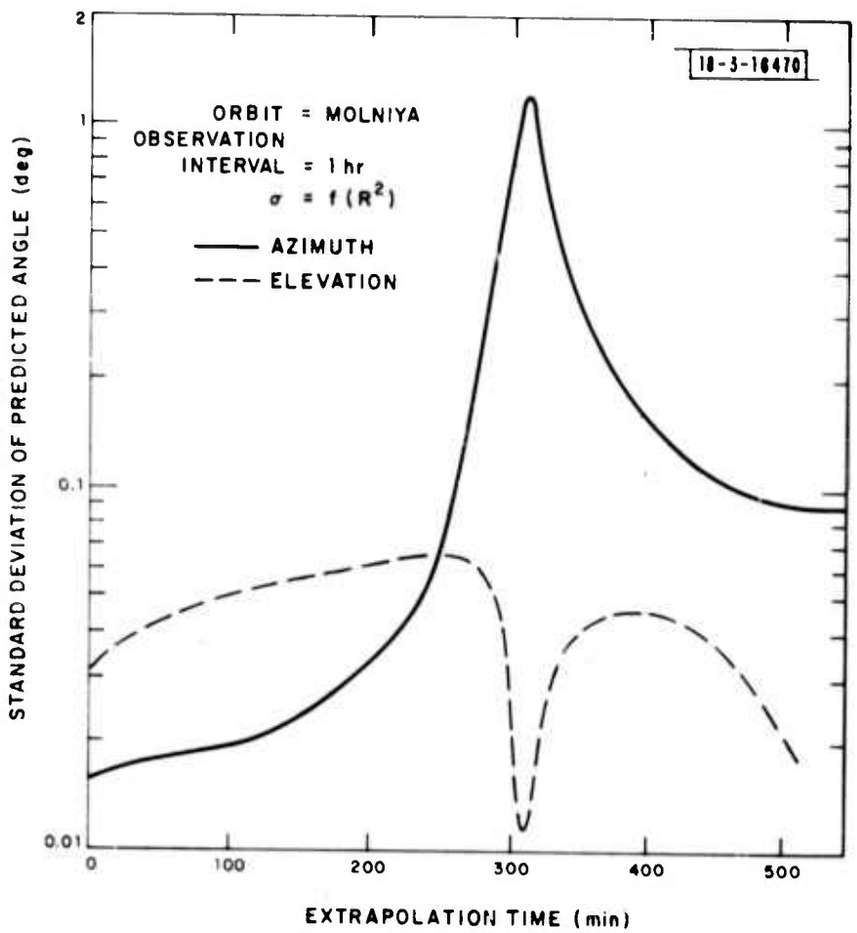

Fig. V-11. RADAR 1 Angle Errors vs. Time

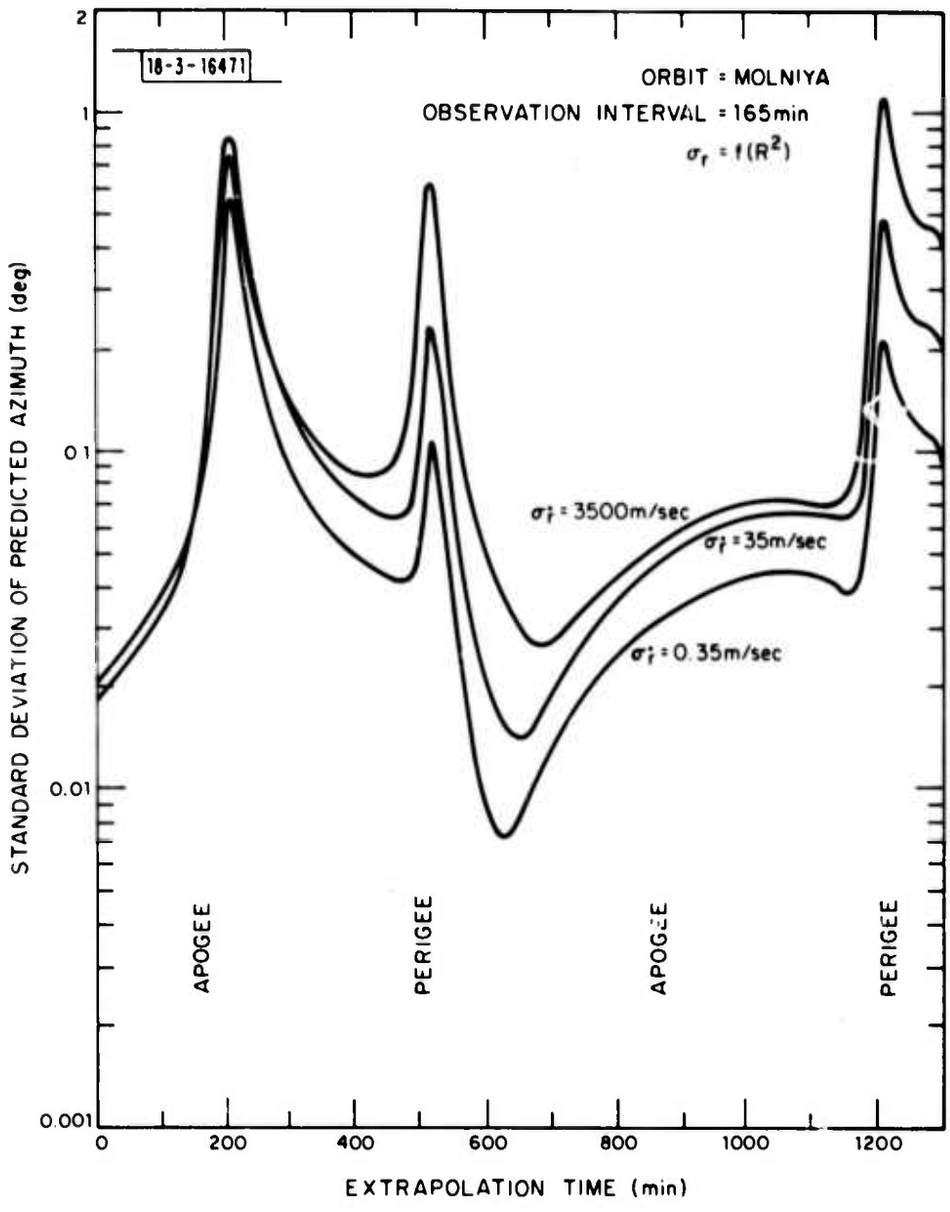

Fig. V-12. RADAR 1 Azimuth Errors vs. Time

obtained when two track intervals of approximately 3 hours separated by one day are used.

E. RADAR 2 Track Data Rate Algorithm

A track data rate algorithm similar to the algorithm described in Section V-B was chosen for use in the error analysis of RADAR 2. The maximum observation interval was limited by the time the satellite remained in the field of view (e.g., 6 hours for a 3 x synchronous altitude orbit). Detection is assumed to occur as the satellite enters the field of view. The radar was arbitrarily placed at 30° N, 230° W with the satellite starting at 30° N, 155° E. The measurement uncertainties are similar to those listed in Table V-1 with the appropriate values substituted for the range, angle and range-rate resolutions. The observation intervals used in the error analysis for the 3 x sync orbit are listed in Table V-8.

TABLE V-8

OBSERVATION INTERVALS (3 x Sync Orbit)

Case Number	Data Rate	Data Interval
1	1 obs/12 sec	1 Hr
2	1 obs/12 sec	1 Hr
	1 obs/5 min	1 Hr
3	1 obs/12 sec	1 Hr
	1 obs/5 min	2 Hr
4	1 obs/12 sec	1 Hr
	1 obs/5 min	3 Hr
5	1 obs/12 sec	1 Hr
	1 obs/5 min	4 Hr
6	1 obs/12 sec	1 Hr
	1 obs/5 min	5 Hr

F. Error Analysis (3 x Sync Orbit; RADAR 2)

Fig. V-14 shows the growth of the error ellipsoid in terms of radar angular coordinates (azimuth and elevation) for the initial data rate and observation interval. After 5 minutes of extrapolation (after a tracking

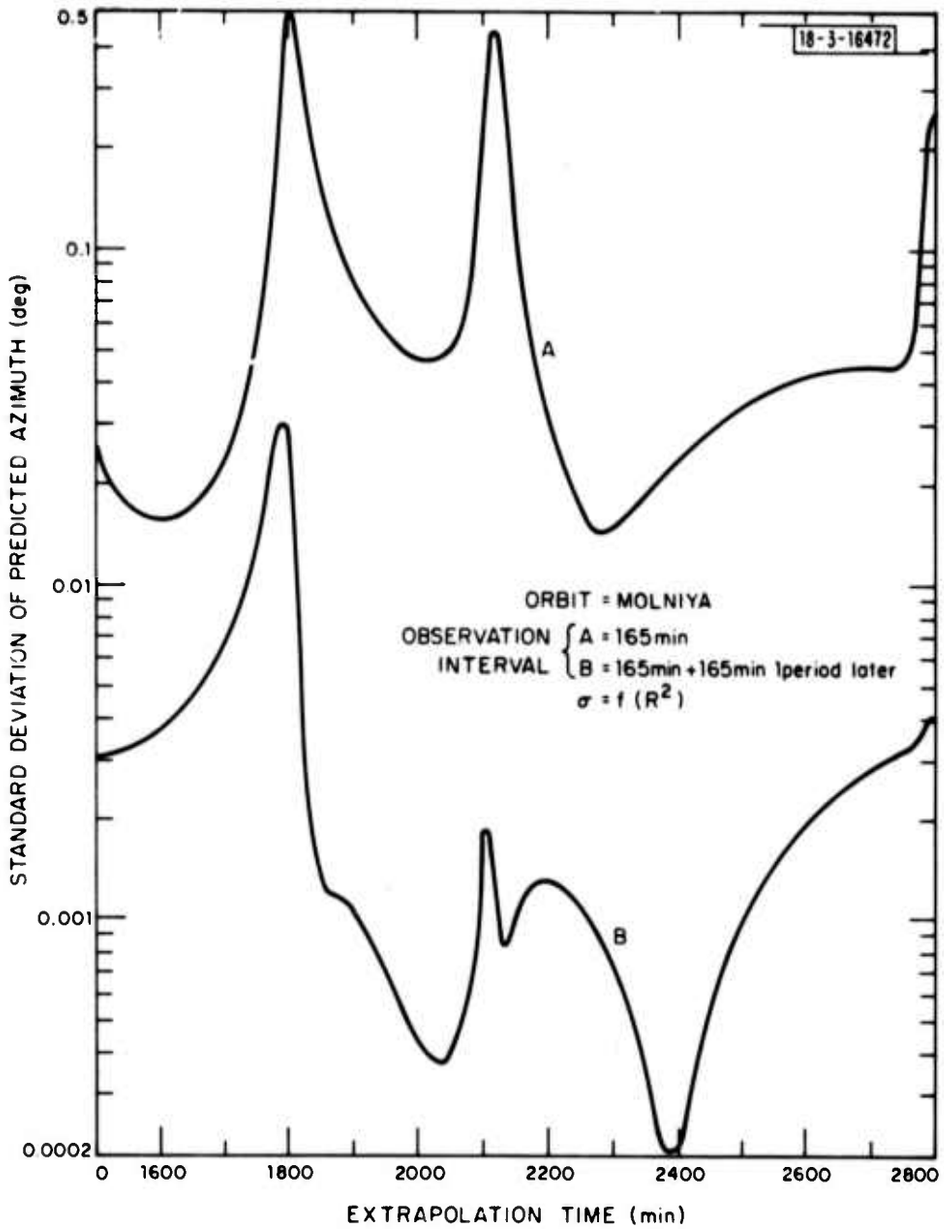

Fig. V-13. RADAR 1 Azimuth Errors vs. Time

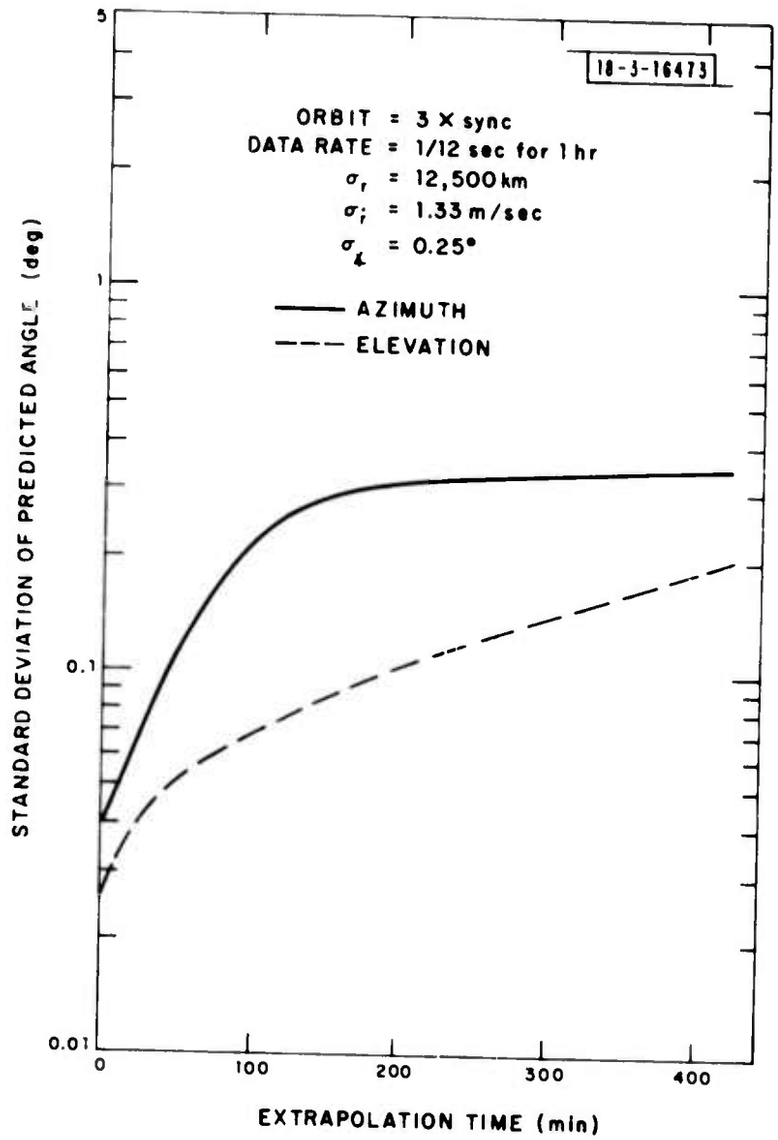

Fig. V-14. RADAR 2 Angle Errors vs. Time

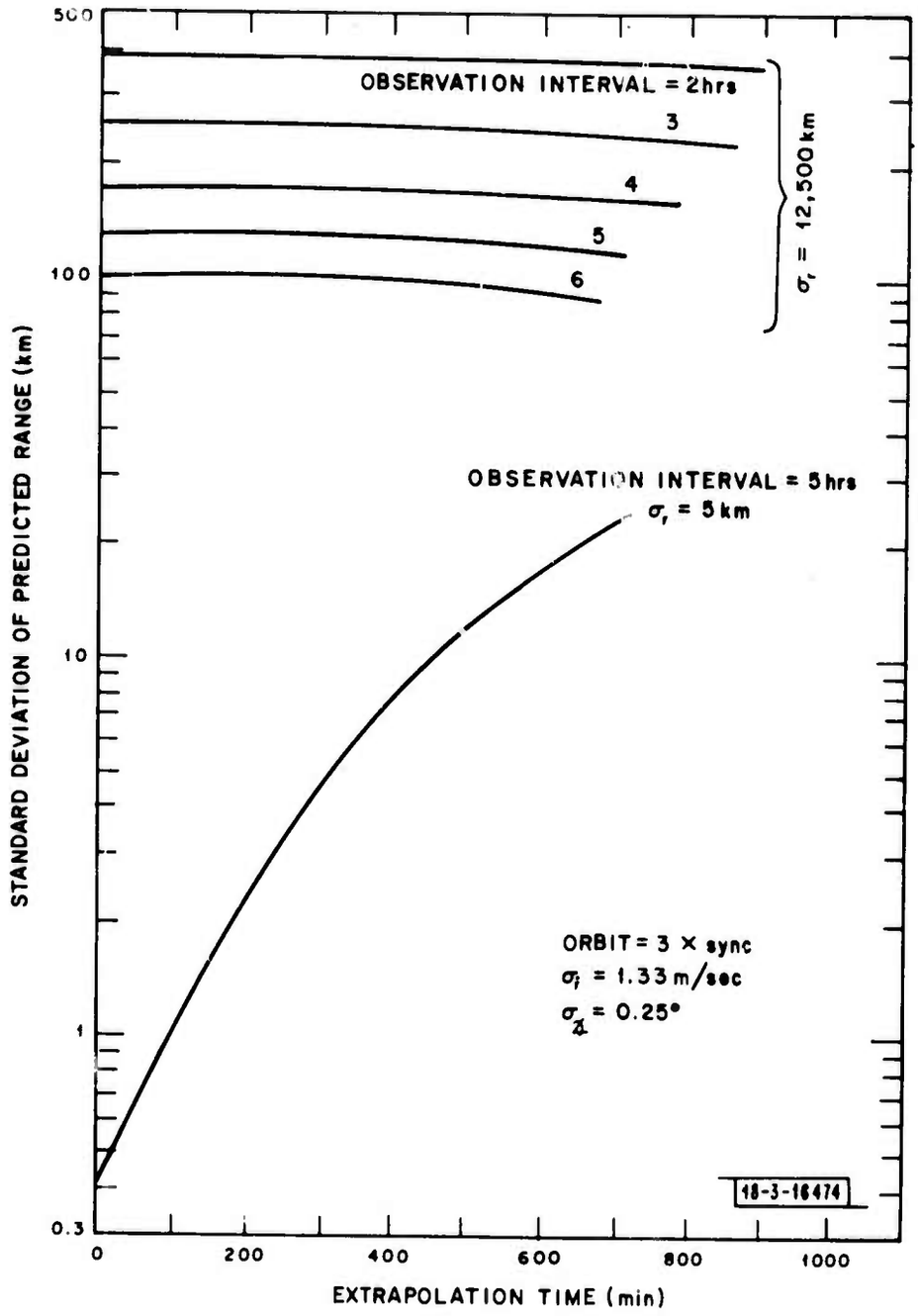

Fig. V-15. RADAR 2 Range Errors vs. Time

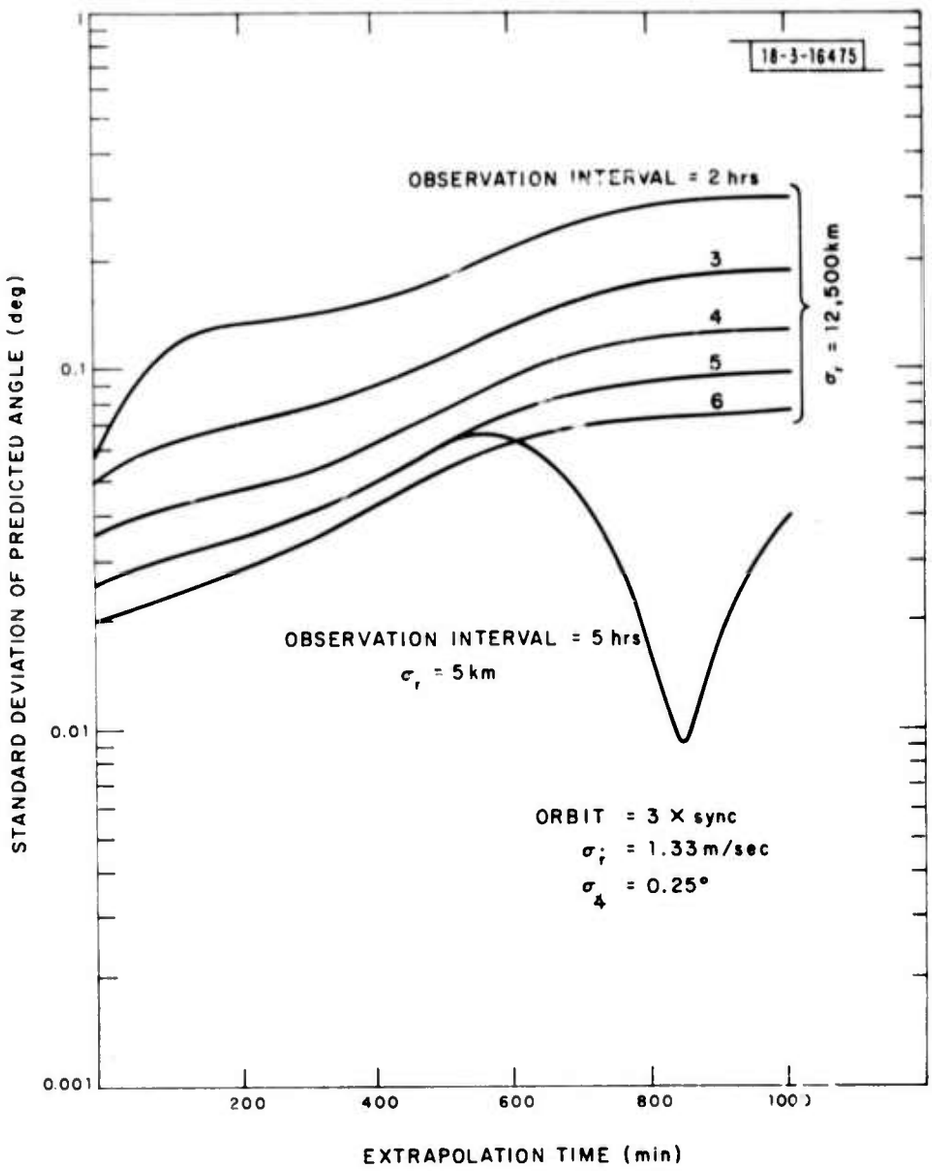

Fig. V-16. RADAR 2 Azimuth Errors vs. Time

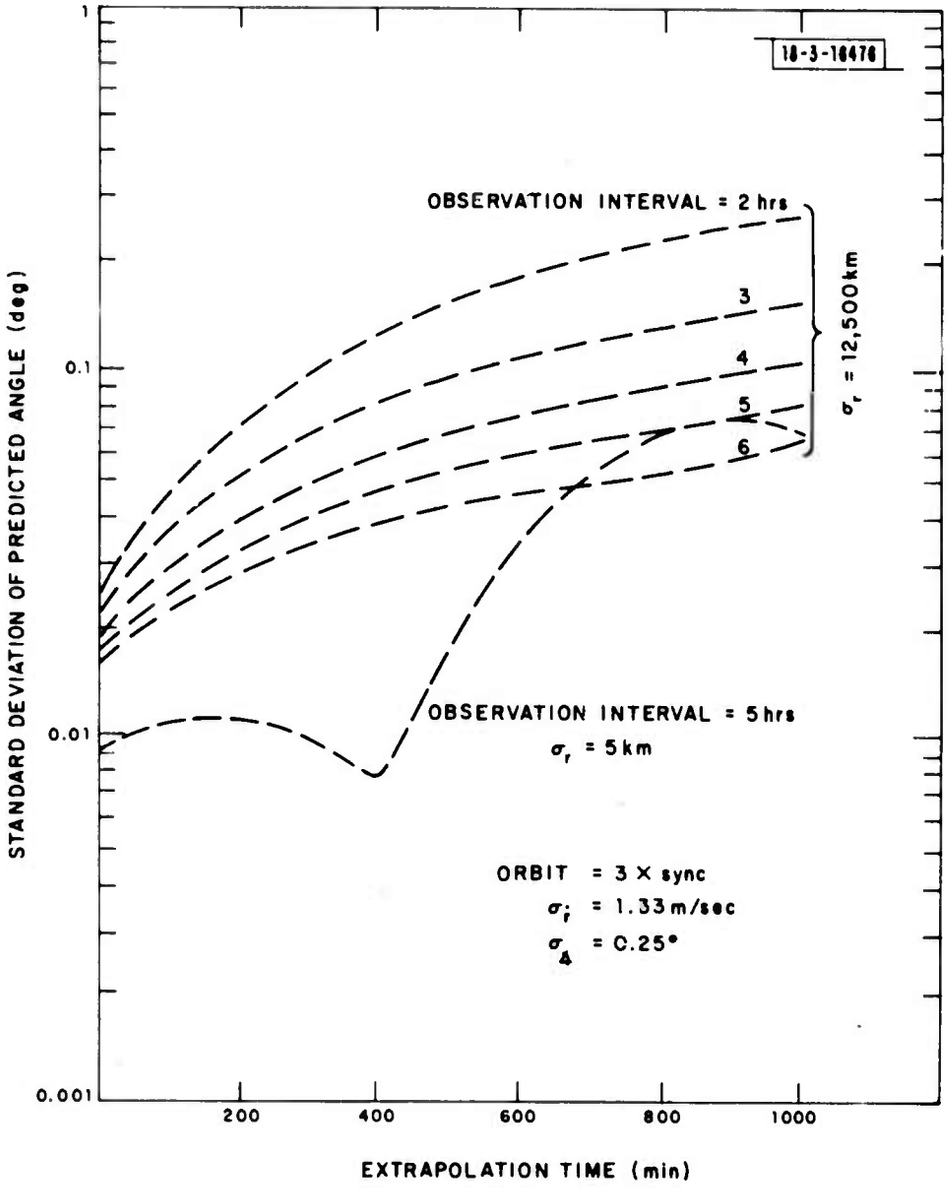

Fig. V-17. RADAR 2 Elevation Errors vs. Time

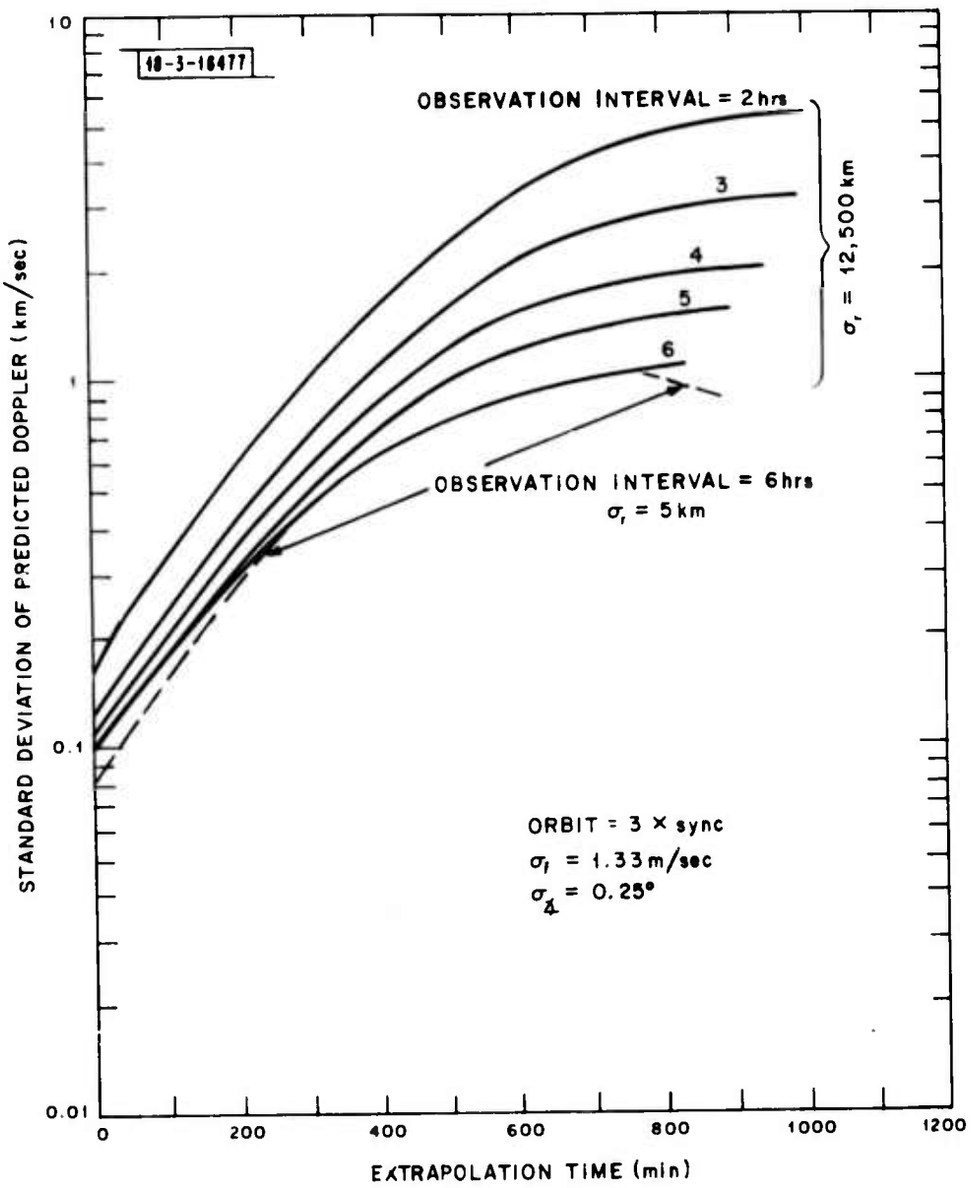

Fig. V-18. RADAR 2 Doppler Errors vs. Time

TABLE V-9

1 σ PREDICTION ERRORS vs. TIME

OBSERVATION TIME	TIME	σ_r (km)	σ_{Az} (Deg)	σ_{El} (Deg)	$\sigma_{\dot{r}}$ (m/sec)
2 Hr.	EOT	400	.06	.03	.16
"	1st Orbit	400	.38	.35	5.5
"	2nd Orbit	700	4.8	3.2	19
"	3rd Orbit	890	11	5.0	26
3 Hr.	EOT	250	.05	.02	.13
"	1st Orbit	250	.22	.21	3.2
"	2nd Orbit	430	2.8	1.9	11
"	3rd Orbit	550	7.1	2.9	16
4 Hr.	EOT	180	.04	.02	.12
"	1st Orbit	180	.15	.14	2.1
"	2nd Orbit	300	1.9	1.3	7.2
"	3rd Orbit	370	4.8	2.0	11
5 Hr.	EOT	130	.03	.02	1.0
"	1st Orbit	130	.11	.10	1.5
"	2nd Orbit	220	1.4	.90	5.2
"	3rd Orbit	280	3.5	1.4	7.6
6 Hr.	EOT	100	.02	.02	.10
"	1st Orbit	100	.08	.08	1.1
"	2nd Orbit	170	1.1	.69	4.0
"	3rd Orbit	220	2.3	1.1	6.0

* 3 x Sync Orbit

Radar 2

Entries are Max. Values during an orbital period (~5 days)

Observation Errors

Range: σ_r = 12,500 km

Angle: $\sigma_{\measuredangle}$ = .25°

Doppler: $\sigma_{\dot{r}}$ = 1.33 m/sec

period of 1 hour) there exists a 99% probability of placing the beam on the target close enough to beam center to insure a maximum loss in S/N of 1 dB. This appears to be a reasonable degradation in signal strength (10%) for maintaining "good" track.

Figs. V-15, 16, 17 and 18 show the growth of the error ellipsoid in the four radar coordinates; range, azimuth, elevation, and range-rate, respectively, as a function of time. Table V-9 summarizes these results and lists the 1 σ errors at the end of track (EOT), and maximum value during the first, second and third orbital period. One orbital period is approximately 5 days. The error analysis shows that, after observing the satellite for the maximum amount of time (6 Hrs.) it is in the field of view, the errors during the second orbital period (10 days) require a small search (4 beam positions) to insure a 68% probability of finding the satellite. A much larger search is necessary to obtain a greater than 99% probability of finding the satellite after 10 days. Table V-10 lists the number of beam positions that must be searched and the search time to obtain a greater than 99% probability of finding the satellite during the second orbital period as a function of track time.

TABLE V-10

SEARCH AREA vs. OBSERVATION TIME
(for >99% probability on 2nd Orbit)

Observation Interval (Hrs.)	Beam Positions	Search Time
2	2300	47 min 8 sec
3	780	16 min 18 sec
4	370	7 min 43 sec
5	190	3 min 54 sec
6	130	2 min 38 sec

Table V-11 lists the number of beam positions that must be searched and the search time to obtain a greater than 99% probability of finding the satellite during the third orbital period (15 days) as a function track of time.

TABLE V-11

SEARCH AREA vs. OBSERVATION TIME
(for > 99% probability on 3rd Orbit)

Observation Interval (Hrs.)	Beam Position	Search Time
2	7920	165 min 0 sec
3	3010	62 min 43 sec
4	1392	29 min 0 sec
5	714	14 min 53 sec
6	392	8 min 10 sec

At three times synchronous orbit, a satellite will remain in the field of view of the sensor for approximately 6 hours. In this case, a much shorter time can be allocated to the reacquisition-search task even though the orbital period is approximately 120 hours. A reasonable amount of time may be, for example, 20 to 30 minutes which would require an initial observation interval of 3 hours if we desired a 99% probability of finding the satellite after two orbits of extrapolation (~ 10 days).

Figs. V-16 and 17 also show the effects of improved range resolution on the extrapolated angular errors when the observation interval is 5 hours. There is no significant improvement in the maximum value of the angular errors. Figs. V-15 and 18 also show the improvement in range and range-rate errors. There is a significant improvement in the range error during the observation interval and immediately thereafter. The long-term improvement is much less significant. There is no significant improvement in the range-rate error.

Fig. V-19 shows the growth of the angular error after 10 days (third orbit) of extrapolation for an observation interval of two hours. This data indicates that caution must be used when the errors are studied at any one instant of time. There is at least an order of magnitude variation of the angular errors. The values listed in Tables V-9 represent the maximum peak during an orbital period.

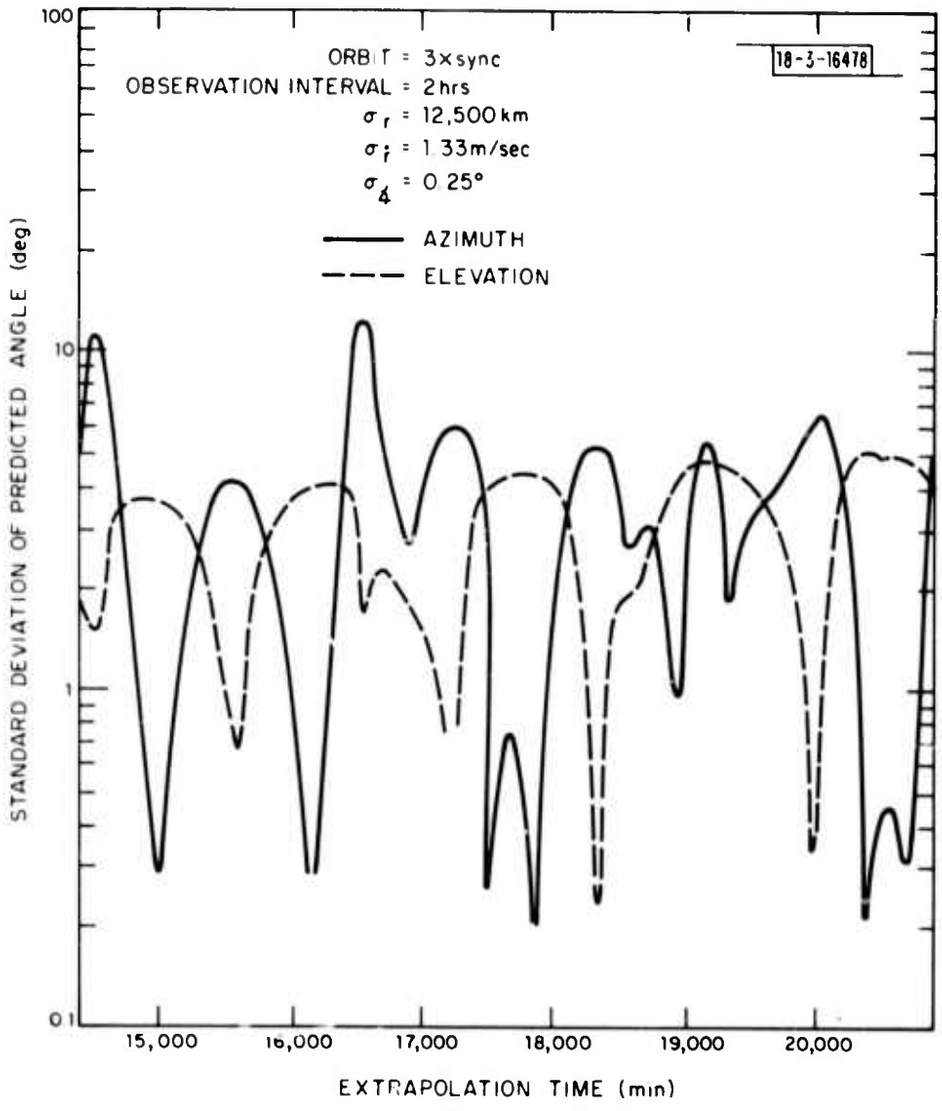

Fig. V-19. RADAR 2 Angle Errors vs. Time

The maximum angular standard deviation during the first orbital period, for an observation interval of five hours, was approximately 0.1 degrees. The $\pm 3\sigma$ value of this error is 0.6 degree which is slightly larger than the 0.5° beamwidth. At the end of the first orbit, it was assumed that the satellite was reacquired and tracked for an additional hour at a data rate of 1 observation every 5 minutes. Figure V-20 shows the improvement in elevation error resulting from the additional observation data. A corresponding improvement (10 times) was evident in the standard deviation of the azimuth errors.

It is not necessary to wait a full orbital period to re-acquire the satellite. The earth's rotation will sweep the radar field of view past the satellites longitude about once every 1.2 days. When the satellite is north of 12.8° S it will be in the radar's field of view. The satellite will spend slightly more than half its period ($\sim$5 days) above this critical latitude. Therefore, in the worst case, it will enter the radar field of view within three days of the last sighting. The above calculations show that the satellite need not be observed during every interval of visibility to maintain a good quality track.

G. Error Analysis (Elliptical Orbit)

In this section, we study the growth of the angular errors resulting from a track of an elliptical orbit whose perigee altitude is 1 x sync and apogee altitude is 3 x sync, i.e., e = 0.5. The radar was arbitrarily placed at 30° N, 160° W with the satellite starting at 215° E. The tracking data rate algorithm is identical to that used in the previous section and the observation interval was arbitrarily set at 5 hrs. The S/N was assumed constant over the observation interval. The range variation during the observation interval was 1.4 to 1 which represents an actual 5.8-dB variation in S/N ratio. Fig. V-21 shows the growth of the angular errors as a function of extrapolation time for a track interval of 5 hours. There is no significant difference between tracking a target in a 3 x synchronous altitude circular orbit and one in an elliptical orbit as described above.

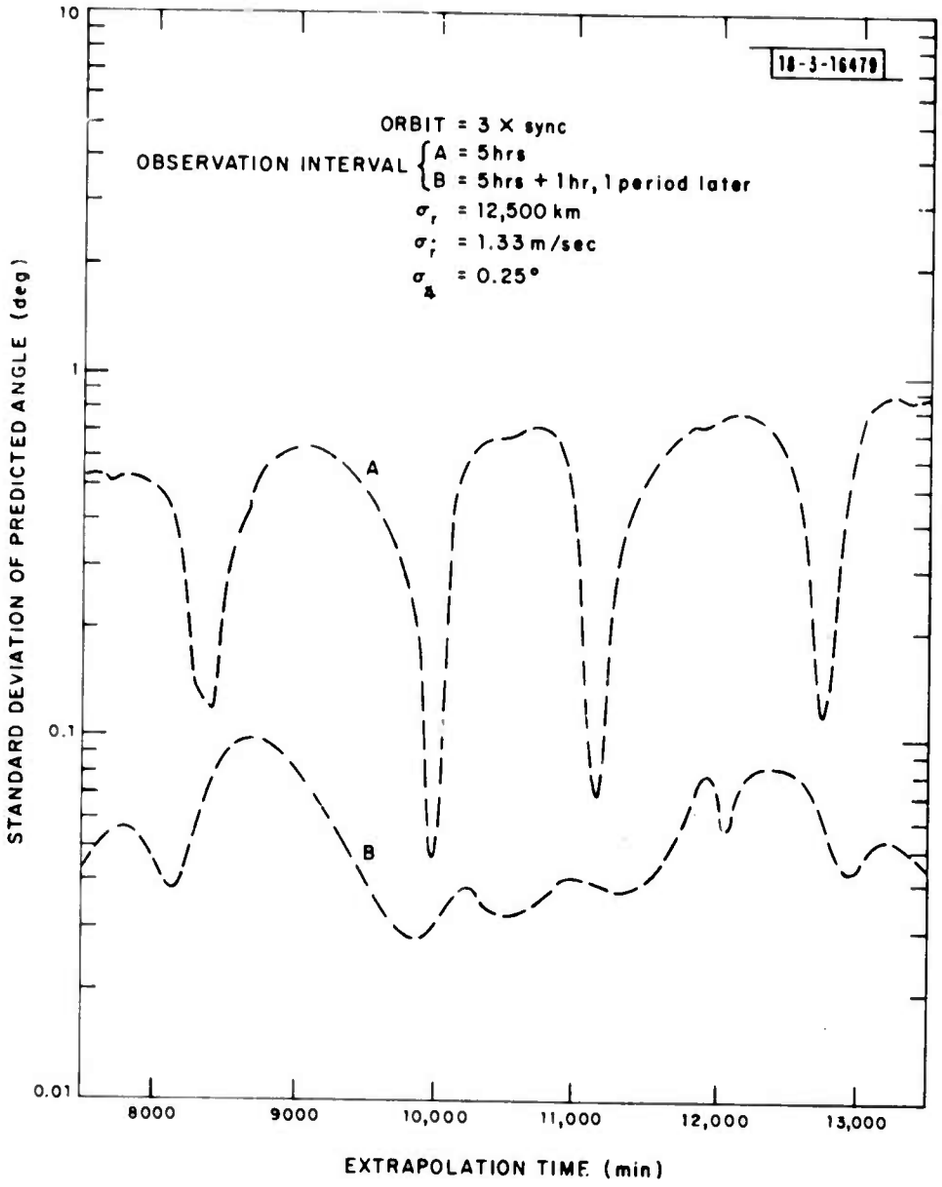

Fig. V-20. RADAR 2 Elevation Errors vs. Time

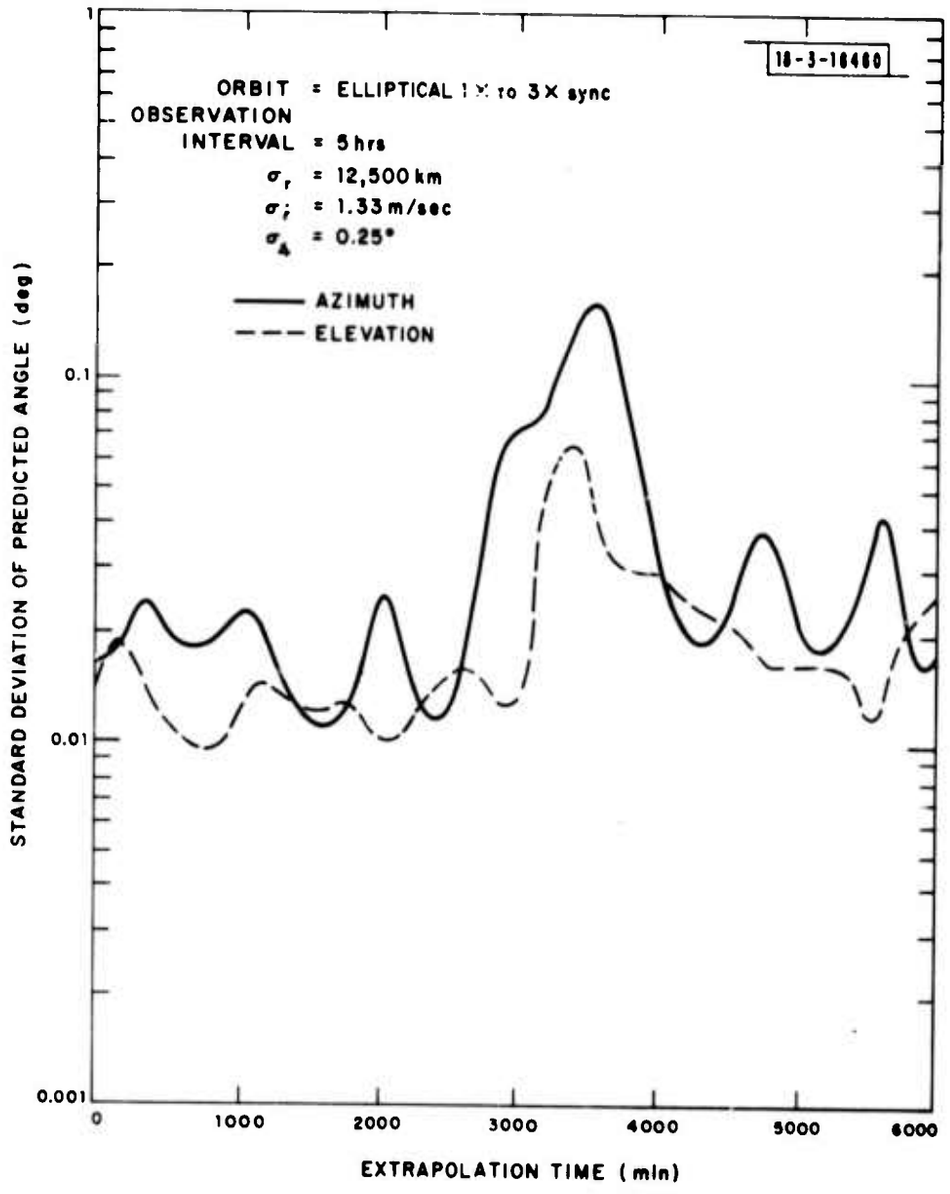

Fig. V-21. RADAR 2 Angle Errors vs. Time

H. Conclusions

The RADAR-1 short-term extrapolation results indicate that the generated ephemeris could be extrapolated for a reasonable fraction of an orbital period for both the 1 x synchronous altitude circular and the highly elliptical orbits. The track data rate algorithms used in the analysis do not represent the optimum use of radar resources, but they were shown to perform the tracking task adequately.

The long-term extrapolation results indicate observation times on the order of 1/4 of the orbital period are required to maintain the extrapolated angular errors within reasonable bounds. A considerable amount of observation time can be saved if a shorter initial track interval is supplemented by one hour of track data one orbital period later.

It was shown that improved range resolution or range-rate resolution decreases the extrapolated angular errors. These errors will also remain within reasonable bounds if the radar is denied either accurate range or range-rate information. If the radar is denied both accurate range and range-rate information, the extrapolated angular errors will become extremely large.

The RADAR-2 short-term extrapolation results were similar to those obtained for RADAR-1. The orbits considered in this case were 3 x synchronous altitude circular and elliptical orbits.

The long-term results indicate the observation interval should be on the order of 1/2 the time the satellite is in the field of view of the radar ($\approx$ 3 hours). A significant improvement in the extrapolated angular errors is realized when an initial observation period of 5 hours is supplemented 1 orbital period later by a 1-hour observation interval.

It was shown that improved range resolution did not have a significant effect on the extrapolated angular errors. The largest improvement was in the short-term extrapolated range error.

The radar systems studied are both capable of developing an ephemeris and are able to recognize and reacquire the satellite on the next orbit by extrapolating the generated ephemeris.

VI. SATELLITE-BORNE ANGLE-ONLY TRACKER ERROR ANALYSIS

A. General

A series of computer simulations were run to evaluate the angular error growth rate as a function of observation time for a sensor located in a geostationary orbit. In each case, the sensor made observations of the target and the orbital parameters were extrapolated for one day. The error analysis propagates the covariance matrix along the trajectory. The results of the error analysis are presented in the sensor's coordinate system (i.e., azimuth and elevation). The accuracy of each measurement was assumed to be 0.05 degree. The results can be scaled to other measurement accuracies directly.

B. Track Data Rate Algorithm

A track data rate algorithm was selected which took one observation every 10 minutes for various observation intervals. Table VI-1 lists the various cases studied.

TABLE VI-1

OBSERVATION INTERVALS

Case Number	Orbit	Data Rate	Number of Observations
1	SYNC	1 obs/10 min.	6
2	SYNC	1 obs/10 min.	12
3	SYNC	1 obs/10 min.	18
4	SYNC	1 obs/10 min.	36
5	2 x	1 obs/10 min.	18
6	3 x	1 obs/10 min.	18
7	Molniya	1 obs/10 min.	18

Figure VI-1 shows the geometry of the satellite-borne sensor and synchronous-altitude target. For this case, the position of the target remains fixed with respect to the sensor since both are in identical orbits. The

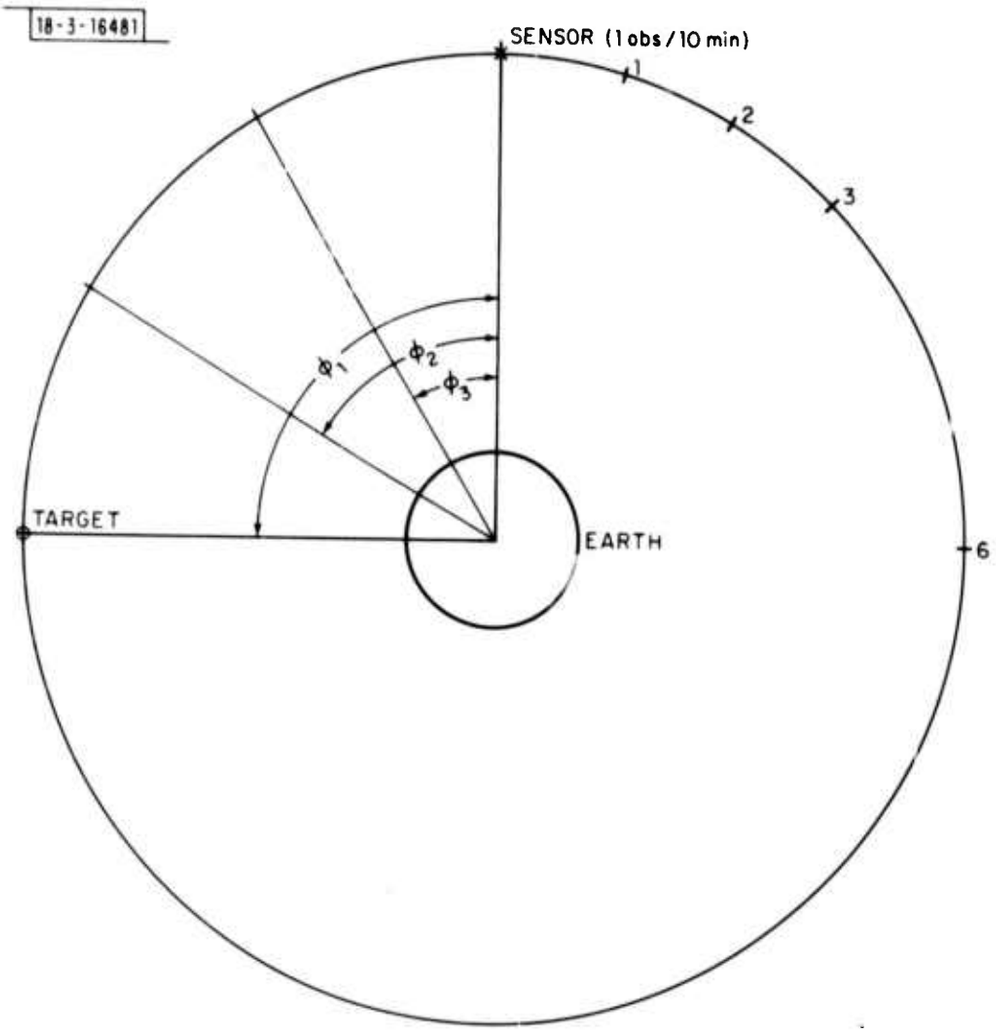

Fig. VI-1. 1 x Sync. Orbit Geometry

angular separation (φ_1) was fixed at 90° for the analysis of the effect of observation interval length on angular errors. Next, the angular separation was varied for a fixed observation interval.

C. Error Analysis (Circular Orbits)

Figure VI-2 shows the growth of the angular errors for various observation intervals. The elevation error grows at a faster rate than the azimuth error component. The azimuth error represents an out of plane error or an error in inclination whereas the elevation error is an in plane error and represents an error in mean anomoly. Table VI-2 lists the extrapolation time when the error exceeds 1 degree.

TABLE VI-2

TIME FOR ERROR TO EXCEED 1°

Number of Observation	Time (min.)
6	35
12	80
18	120
36	360

There is a significant increase in the time for the error to exceed 1 degree when the number of observations increases from 18 to 36. The target satellite moves 0.25 degrees/minute and during the longest observation interval moves 87.5 degrees of central arc.

Fig. VI-3 shows the angular errors vs. extrapolation time as a function of position of the target in the orbit relative to the sensor. The results show that the errors are nearly independent of the relative position of the target and sensor. The analysis shows that if reasonable angular errors are to be achieved, the satellite must be observed over approximately 90° of its orbit ($\approx$ 360 min.).

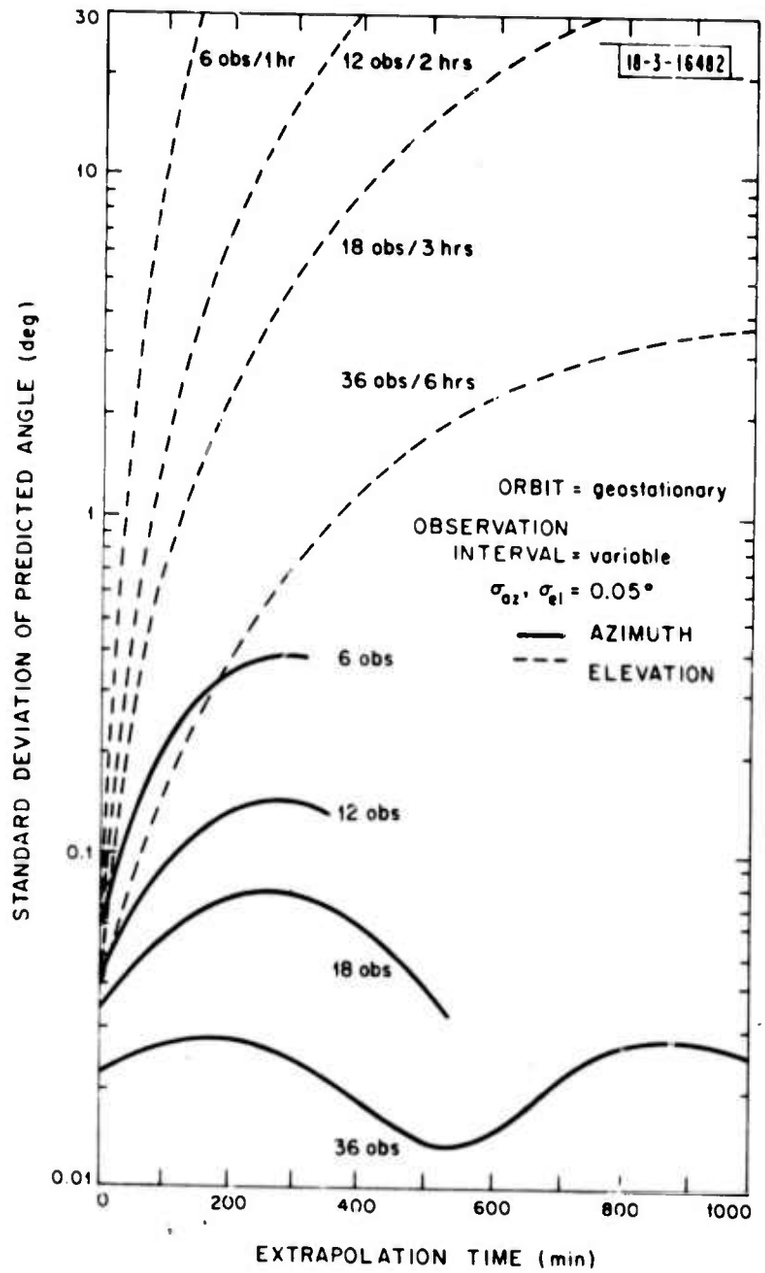

Fig. VI-2. Satellite Sensor Angle Errors vs. Time

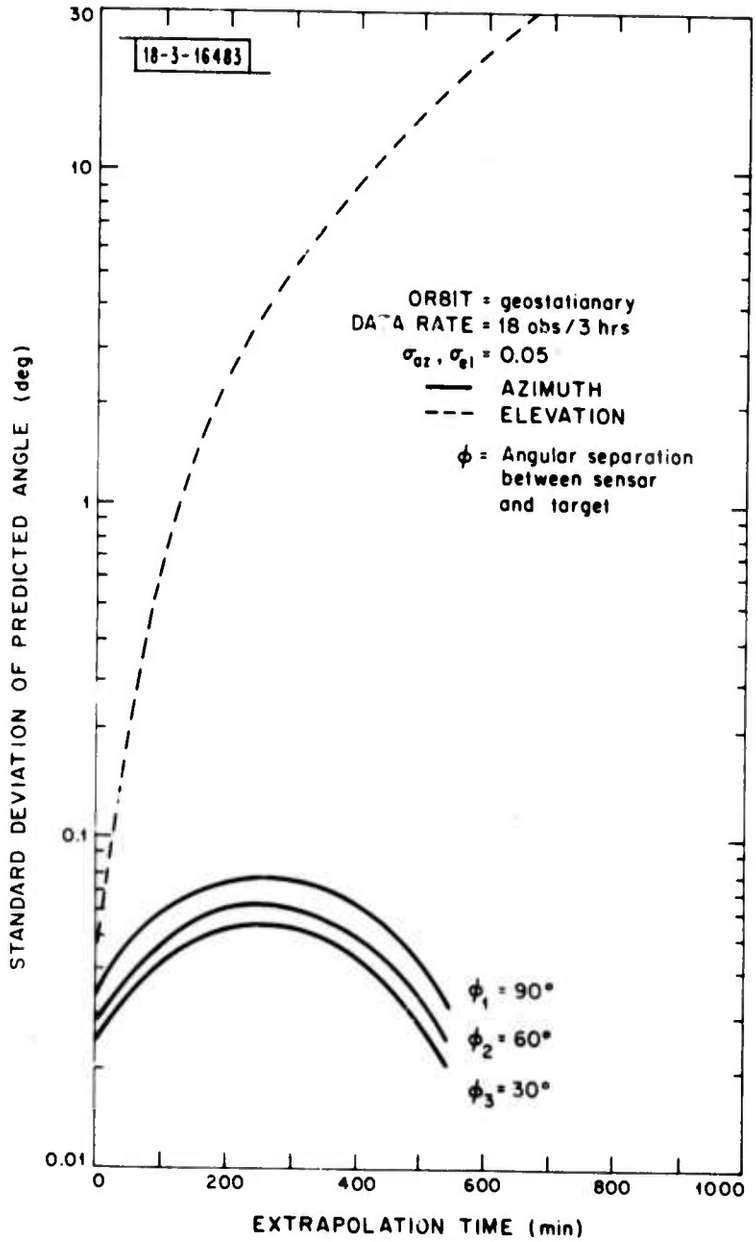

Fig. VI-3. Satellite Sensor Angle Errors vs. Time

D. Error Analysis (Other Orbits)

The analysis was extended to cover three other orbits, i.e., 2 x sync, 3 x sync, and a typical Molniya orbit. Figs. VI-4, 5 and 6 show the resulting angular errors as a function of extrapolation time. The data rate was 1 observation every 10 minutes and a total of 18 observations were used in all cases. The azimuth and elevation errors grow with approximately the same rate in all cases and the magnitudes of the errors are similar. The curves are self explanatory in view of the previous discussions.

E. Conclusions

The satellite-borne angle-only sensor short-term extrapolation results for the geostationary orbit indicate that reasonable angular errors can be achieved if the satellite is observed for approximately 90° of its orbit (≈ 6 hours). Additional cases should be studied to extend the short-term results.

Simulated observations were made of satellites in 2 x and 3 x synchronous altitude circular orbits and an elliptical orbit. The results for these orbits are all similar and show that reasonable errors can be expected for observation intervals which cover approximately 3 hours. Longer observation intervals will reduce the extrapolated errors.

It is clear from the analysis that this sensor has the capability to generate an ephemeris and should be able to recognize the satellite on the next orbit by extrapolating the generated ephemeris.

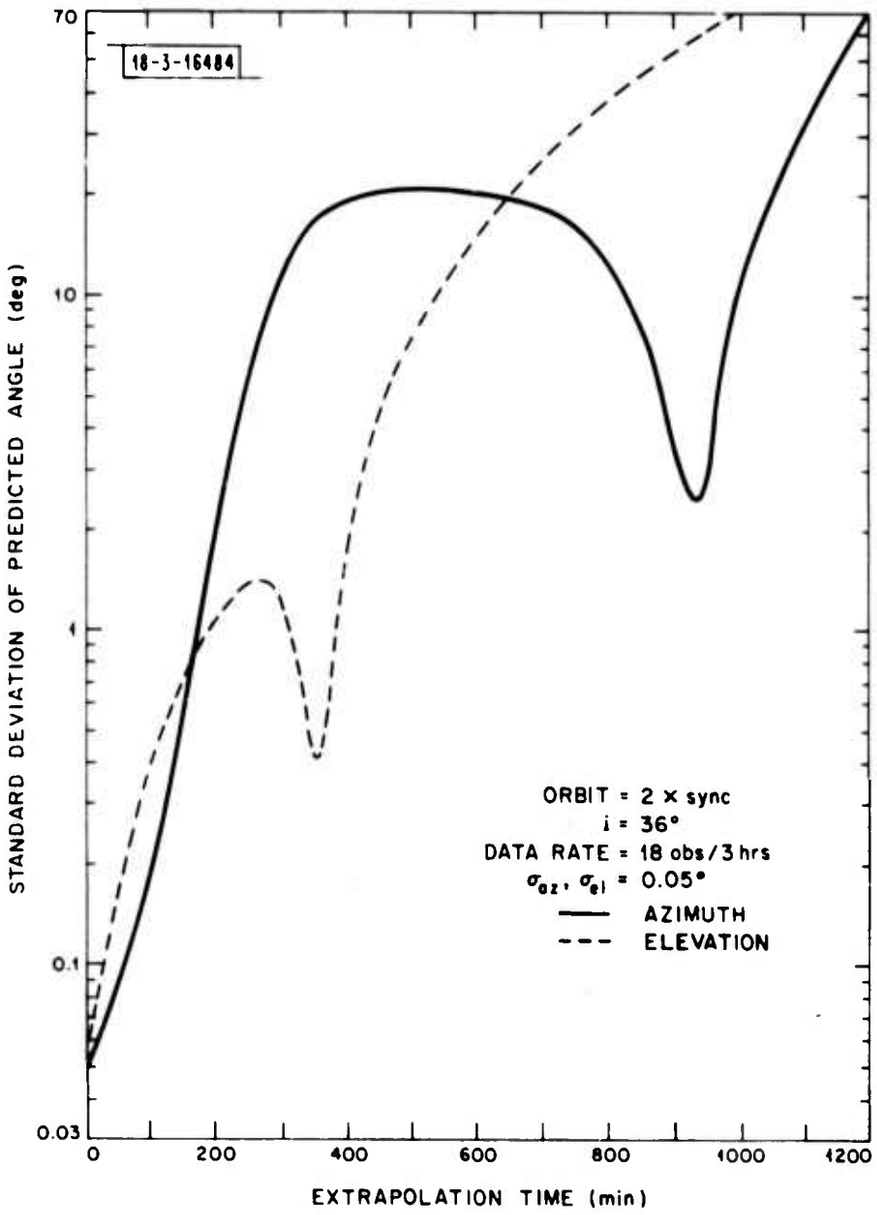

Fig. VI-4. Satellite Sensor Angle Errors vs. Time

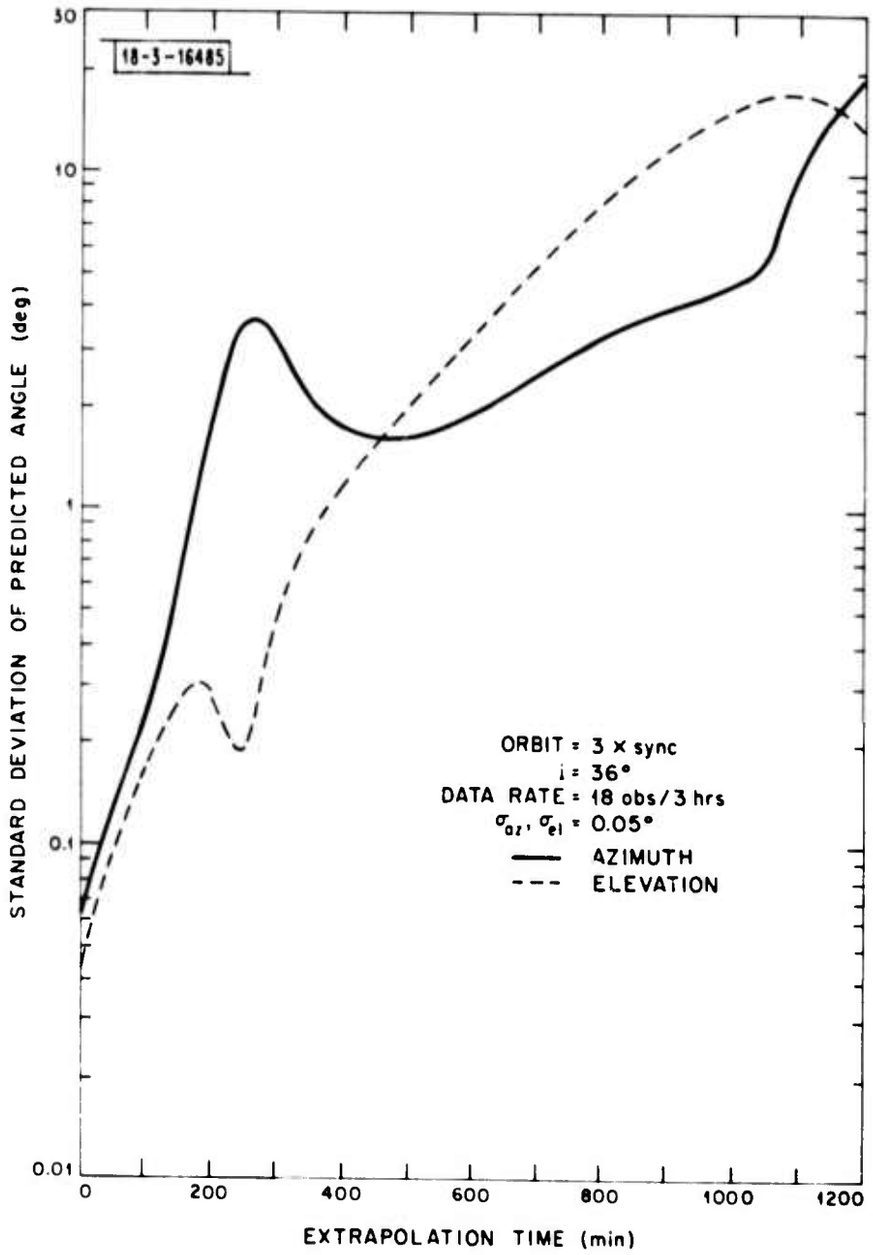

Fig. VI-5. Satellite Sensor Angle Errors vs. Time

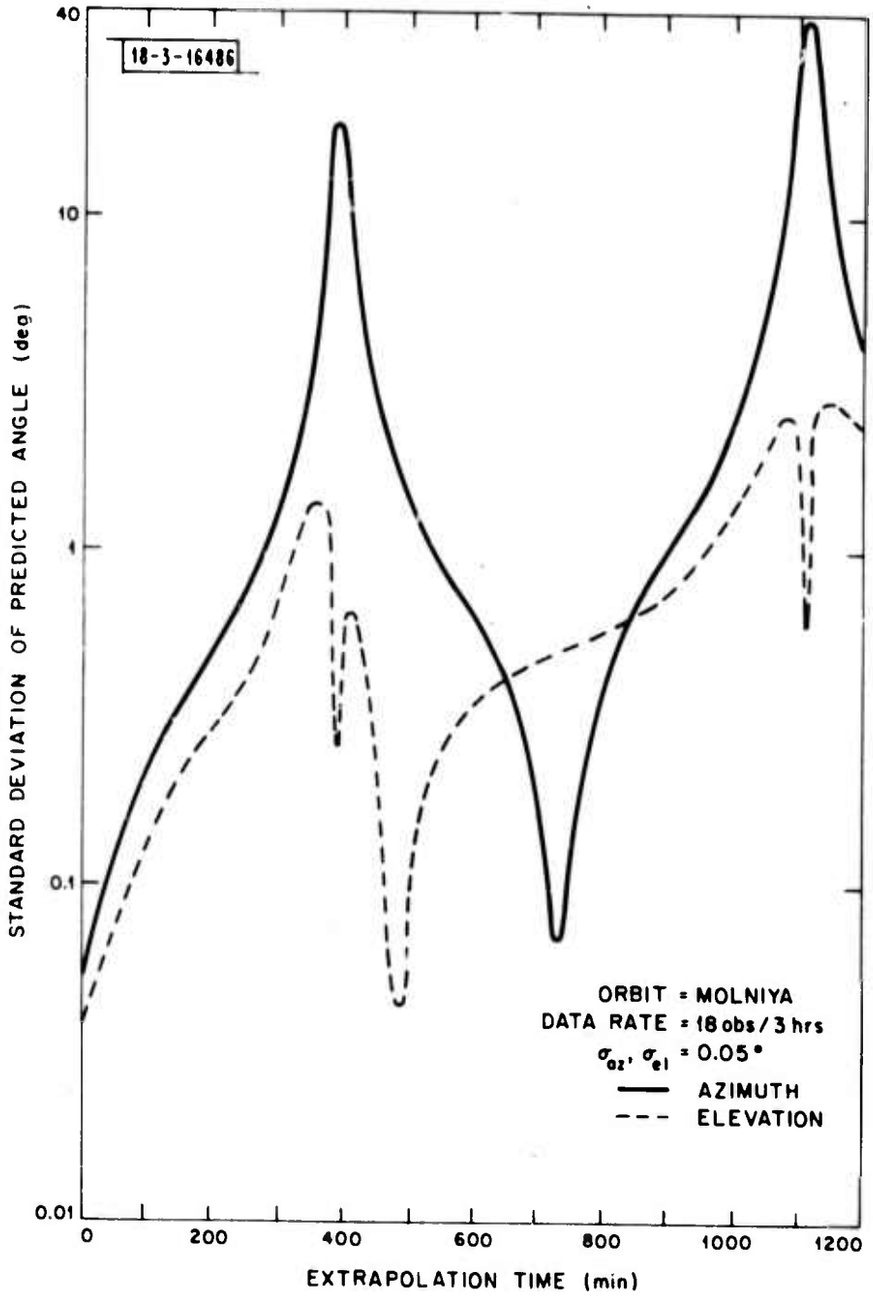

Fig. VI-6. Satellite Sensor Angle Errors vs. Time

APPENDIX I

SCALING RULES FOR RESULTS OF ERROR ANALYSIS

This appendix gives a few scaling rules that can extend the usefulness of the error analysis results in this paper to other cases. A great deal has been written (see for example references 1 and 2) about such scaling rules and other approximations that are amenable to hand calculation. In this appendix we will restrict ourselves to rules that can be simply stated and for which conservative limits of applicablility have been derived from basic principles. These caveats are a most important part of any formulation of scaling rules.

To apply any of these scaling rules one must hold the satellite orbit and sensor geometry fixed. Only the parameters of the system that are explicitly mentioned in the scaling rules are allowed to vary. To change orbits or sensor locations, new computer runs must be made. All scaling rules require reasonably small prediction errors.

In the following we will assume that the user wishes his error estimates to be accurate to within a factor of 1.5 or 2. Of course, the scaling accuracy can be much better where the inequality constraints are strongly satisfied.

The first scaling rule states that if, all else remains constant, the observational error standard deviations are all multiplied by a common factor, k, then the standard deviation of all predicted position and velocity components will also be multiplied by the same factor, k.

This rule follows from the fact that for small observational errors, the prediction errors are linear functions of the observation errors. This linearity condition is also the basis for the error analysis calculated by the NRTPOD computer program, and it is strongly satisfied in most cases studied in this report.

Only where the scaled prediction errors amount to tens of degrees in angle or many thousands of kilometers in range, for the high-altitude orbits of this study, need one be concerned about the accuracy of this scaling rule. If one does wish quantitative error analyses in such cases, the linear error analyses of NRTPOD should be checked by NRTPOD orbit fits on simulated data containing simulated observation errors. Even for extremely large errors, this scaling rule correctly predicts the outcome of the NRTPOD linear error analysis.

A corollary to the first scaling rule states that if some observational standard deviations are scaled by a factor, k_1, and others are scaled by a factor, k_2, any prediction standard deviation will be scaled by a factor between k_1 and k_2 in magnitude.

Different prediction components may have different scaling factors, but all will fall within this range. An example where this rule might be useful would be where k_1 (applying to all range measurements) and k_2 (applying to all angle measurements) differ by less than a factor of 2. Then if one uses the geometric mean $\sqrt{k_1 k_2}$ as the estimated scaling factor, the scaled prediction standard deviations would all be correct to better than the factor $\sqrt{2}$.

The second scaling rule states that if one scales the data rate, r, by the factor k, keeping constant the time intervals during which data is taken as well as all other parameters of the problem, then the prediction standard deviations all scale as $1/\sqrt{k}$.

This rule requires reasonably small prediction errors and that both initial and final data rates be reasonably high. Eight data points in a single observation interval are usually more than sufficient. The theoretical justification depends on the approximate equality of sums over smoothly varying terms to corresponding integrals. (Reference 1, pp 91-92, for example, derives this rule.)

The third scaling rule states that the prediction errors scale as $t^{-3/2}$ where t is the length of the short tracking interval, under the following conditions:

(a) The prediction time, T, plus the tracking time, t, is less than about a tenth of the orbital period, P, i.e.,

$$T + t \lesssim \frac{1}{10} P \quad .$$

(b) $T > 0$

(c) Only position observations (i.e., range and angle) are used.

(d) The data rate, r, is high and constant, i.e., $rt \gtrsim 8$.

(e) The tracking interval, t, is further limited so that the sensor line of sight does not rotate appreciably in inertial space during t. This can be stated quantitatively as

$$\Delta\theta \lesssim \sigma_R / (R\sigma_\theta)$$

where $\Delta\theta$ is the rotation of the sensor line of sight direction, σ_R is the range standard deviation, R is the range and σ_θ is the angle standard deviation. All angles are in radians.

Condition (a) assures that the gravitational acceleration acting on the satellite is approximately constant in magnitude and direction over the orbital arc. The rectangular components of position in inertial space are approximately decoupled in the equations of motion. Also displacements from the true orbit are linear functions of time with corresponding velocity component errors as the linear coefficients. With positive prediction times, the prediction errors are mostly controlled by the errors in velocity estimation at the midpoint of the track. It is these velocity estimation errors that scale as $t^{-3/2}$ under conditions (c), (d), and (e). Condition (e) is of special note because it permits the choice of a coordinate system aligned with the sensor line of sight in which the error components are statistically as well as dynamically decoupled.

If we combine scaling rules two and three we obtain as a corollary that if we hold the total number of observations constant instead of the data rate as we vary the tracking interval, the prediction errors scale as t^{-1}.

All the other conditions of rule three except (d) must still be satisfied.

Thus one gets most of the benefit of a longer track without the penalty in sensor resources if one takes data at a lower rate over the longer period of time. This t^{-1} scaling result of course applies to the estimated velocity error at the midpoint of the track, and thus it also applies to many predicted position components for all prediction times.

The fourth scaling rule states that the prediction errors scale linearly with the prediction time, T, under the following conditions:

i) $T + t \lesssim \frac{1}{10} P$

ii) $T \gtrsim \sqrt{\frac{t^2}{4} + \frac{\sigma_R}{\sigma_{\dot{R}}^2}} - \frac{t}{2}$

iii) Prediction error components for different T must be compared in a coordinate system that maintains a fixed orientation in inertial space.

Condition (i) is the same as condition (a) of scaling rule three. Condition (i) insures that position displacements from the true orbit caused by velocity errors grow linearly with time in the inertial system of condition (iii) while condition (ii) makes velocity estimation errors predominate. With infinite Doppler errors, condition (ii) reduces to condition (b) of rule three. Conditions (c), (d), and (e) of rule three are not necessary here because in scaling rule four we are no longer concerned with the cause of the estimated velocity error ellipsoid. We are only concerned with propagating the position errors that result from it.

ACKNOWLEDGMENT

The authors are deeply indebted to Dr. H. M. Jones for reviewing the original manuscript and contributing the appendix on scaling rules.

REFERENCES

1. I. I. Shapiro, "The Prediction of Ballistic Missile Trajectories from Radar Observations," Lincoln Laboratory Monograph (McGraw-Hill, New York, 1958).

2. F. C. Schweppe, "Re-entry Trajectory Estimation Error Analysis," not generally available.